All Optical Reflectivity Modulation Utilizing Surface Plasmon Resonance

by

Umar Mohammed Johar

A Thesis Presented to the

FACULTY OF THE COLLEGE OF GRADUATE STUDIES

KING FAHD UNIVERSITY OF PETROLEUM & MINERALS

DHAHRAN, SAUDI ARABIA

In Partial Fulfillment of the
Requirements for the Degree of

MASTER OF SCIENCE

In

ELECTRICAL ENGINEERING

December, 1992

Order Number 1354071

All optical reflectivity modulation utilizing surface plasmon resonance

Johar, Umar Mohammed, M.S.

King Fahd University of Petroleum and Minerals (Saudi Arabia), 1992

U·M·I
300 N. Zeeb Rd.
Ann Arbor, MI 48106

ALL OPTICAL REFLECTIVITY MODULATION UTILIZING SURFACE PLASMON RESONANCE

BY

UMAR MOHAMMED JOHAR

A Thesis Presented to the

FACULTY OF THE COLLEGE OF GRADUATE STUDIES

KING FAHAD UNIVERSITY OF PETROLEUM & MINERALS

DHAHRAN, SAUDI ARABIA

In Partial Fulfillment of the

Requirements for the Degree of

MASTER OF SCIENCE

In

ELECTRICAL ENGINEERING

December, 1992

KING FAHAD UNIVERSITY OF PETROLEUM & MINERALS
DHAHRAN 31261, SAUDI ARABIA

COLLEGE OF GRADUATE STUDIES

This thesis, written by ***UMAR MOHAMMED JOHAR*** under the direction of his Thesis Advisor and approved by his Thesis Committee, has been presented to and accepted by the Dean of the College of Graduate Studies, in partial fulfillment of the requirements for the degree of ***MASTER OF SCIENCE.***

Thesis Committee

Dr. S. J. AL-BADER
Thesis Advisor

Dr. H. A. JAMID
Member

Dr. E. E. HASSAN
Member

Dr. Y. ABDUL-MAGID
Member

Department Chairman

Dean, College Graduate Studies

30.12.92
Date

This thesis is dedicated to my beloved parents for all what they have done for me.

It is also dedicated to all my brothers and sisters.

To those whom i share their care and concern.

ACKNOWLEDGMENT

First of all, praise be to *ALLAH* whose help made it possible to complete this research.

Acknowledgment is due to King Fahad University of Petroleum and Minerals for supporting this research.

I wish to express my appreciation to my principle advisor, Dr. Samir J. Al-Bader for his careful guidance and encouragement through this research. I would also like to express my deep appreciation to my thesis committee member, Dr. Husain A. Jamid for his constant help and encouragement.

I also wish to thank my other committee members Dr. Essam E. M. Hassan and Dr. Youssef L. Abdel-Magid for their help.

Thanks is also to all electrical engineering faculty and students for their constant encouragements.

Finally, special thanks to my parents, brothers, and sister for their encouragement, inspiration and unselfish support during my studies.

خلاصة الرسالة

اسم الطالب الكامل : عمر محمد جوهر .

عنوان الدراســـة : تعديل انعكاسية شعاع من الضوء باستخدام شعاع آخر مستغلاً طنين البلازمونات السطحيه ..

التخـــصـــص : هندسة كهربائية

تاريخ الشهـــاده : ديسمبر ١٩٩٢م

ان الهدف من هذه الرسالة هو برهنه امكانيه تعديل انعكاسيه شعاع من الضوء باستخدام شعاع أخر . وللتوصل لهذا الهدف فقد استخدم طنين البلازمات السطحيه التي تهيج في بنيه كريتشمان المشهورة عندما تكون زاوية الإسقاط مناسبة ويتكون الشكل المقترح من طبقة معدنية رقيقة رسبت على قعر عدسه ذات انعكاسية عاليه . ويحتوي كذلك عال طبقة من ماده غير خطيه قابلة للتشبع مع زيادة المجال الكهربائي الموجود في داخل هذه الطبقة ، توجد هذه الطبقة تحت الطبقة المعدنية . فإذا أسقط شعاع من الضوء ذات متجه المجال المغناطيسي عمودي على السطح الموجود بين العدسه والطبقة المعدنية وكانت زواية الإسقاط مناسبة فإن بلازمون سطحي سوف يهيج على السطح بين الطبقة المعدنية والطبقة الغير خطية . ولنفرض الان ان شعاع اخر اسقط على الشكل من الجهه السفلية (الشعاع المعدل) فإن انعكاسية الطبقة الغير خطيه سوف تتغير مما ينتج عنه خروج البلازمون المهيج عن طنينه . وهذا يعني ظهور الضوء المنعكس من الشعاع العلوي الذي كان مختفياً حين تهيج البلازمون . وقد أفترض في هذا البحث ان الشعاع السفلي فقط يوثر على الطبقه الغير خطيه . وقد درس في هذا البحث العلاقه بين شدت الشعاع السفلي وإنعكاسيه الشعاع العوي . بالاضافه لهذا فقد درس تأثير زواية الاسقاط الشعاع العلوي على انعكاسيته . كما بحثنا تأثير مستوى التشبع على التعديل وأخيراً فإن إمكانيه استخدام الطريقة المسمى المتوافق الذاتي مع موجات ذات مجال مغناطبيسي عمودي على السطح درست في هذا البحث .

درجة الماجستير في العلوم
جامعة الملك فهد للبترول والمعادن
الظهران ، المملكة العربية السعودية
ديسمبر ١٩٩٢م

THESIS ABSTRACT

UMAR MOHAMMED JOHAR

All-Optical Reflectivity Modulation Utilizing

Surface Plasmon Resonance

MAJOR: **Electrical Engineering**

DATE : **December, 1992**

The purpose of this thesis is to demonstrate an all optical reflectivity modulator that utilize surface plasmon resonance. The configuration of the structure is the well known Kretschmann configuration. It consists of a thin metallic layer deposited on the base of a high index prism. A region of saturable nonlinear medium exists under the metallic layer. A TM-polarized light (light to be modulated) is incident into the structure from the prism side and the modulating light is incidence into the structure from the bottom. It was assumed that only the modulating beam affects the nonlinear medium. Relationship between the intensity of the lower beam and the reflectivity was studied. In addition, the effect of changing the angle of incidence of the upper beam on the reflectivity was investigated. Furthermore, the effect of increasing the saturation level on the modulation was investigated. The applicability of the self-consistent approach for TM-polarized waves was also discussed.

MASTER OF SCIENCE DEGREE
KING FAHAD UNIVERSITY OF PETROLEUM AND MINERALS
Dhahran, Saudi Arabia
December, 1992

TABLE OF CONTENTS

LIST OF FIGURES

Figure *Page*

CHAPTER 1

GENERAL INTRODUCTION

1.1 INTRODUCTION

The use of optical fibers in high speed communication gave rise to many devices that operate at optical frequencies. In this thesis, an all optical modulator is proposed and analyzed. All optical modulation means that the information imbedded in a beam of light is transformed to another beam. The modulator utilizes surface plasmon resonance and material nonlinearity.

Although any electromagnetic wave contains six components, three electric field components and three magnetic field components, they can

be divided into two groups called TE (transverse electric) and TM (transverse magnetic) waves in a planar structure. The criterion that differentiate TE waves from TM waves is that in the TE case no electric component exists in the direction of propagation and the single electric component is parallel to the interfaces of the wave guide. On the other hand, in the TM case there is only one magnetic component which is perpendicular to the direction of propagation and parallel to the interfaces of the wave guide. There has been increasing interest in recent years in TM and TE waves and it has been shown that the interface between metal and dielectric and the interface between a linear and nonlinear medium supports TM polarized surface waves [1].

Assume an obliquely incident TM - polarized plane wave is reflected from a surface of a thin metallic film backed by a nonlinear dielectric layer. Since the dielectric constant of the nonlinear medium is dependent on the field present in the layer, the reflected field can be modulated by a second plane wave incident normally on the nonlinear layer of the suggested structure on the opposite side.

Consider the structure shown in figure (1.1), and assume that a TM-polarized plane wave having a low intensity is incident from a dielectric medium with refractive index n_p on the upper surface of a thin metallic

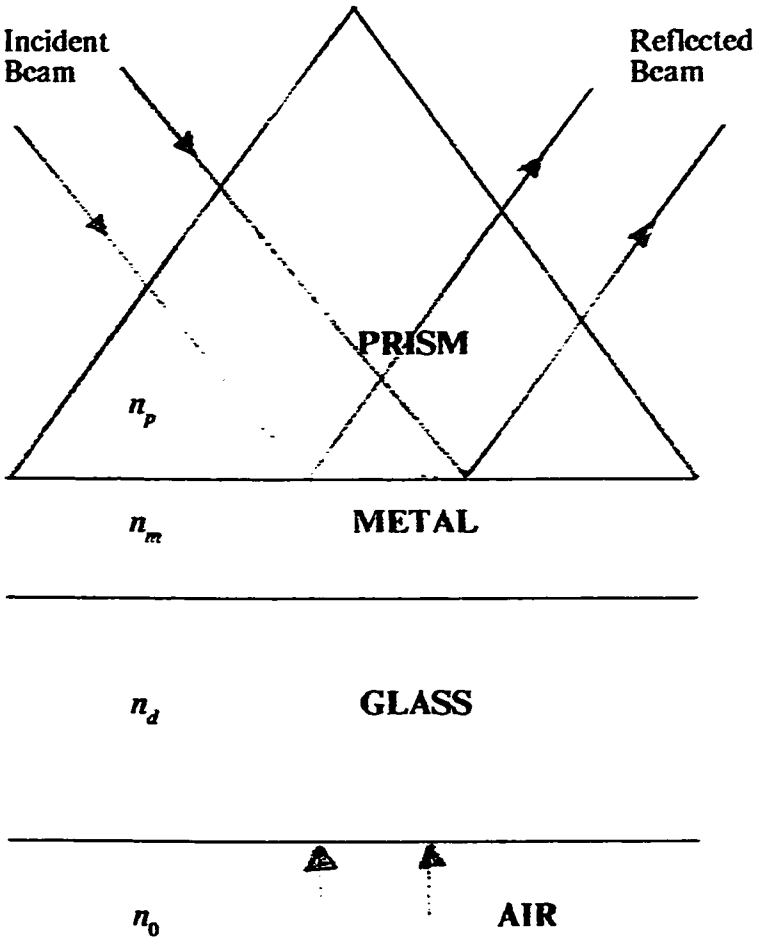

Figure (1.1) The structure used for reflectivity modulation using a normally incident beam.

film of dielectric constant n_m^2 and thickness t. The metallic film is assumed to be backed by a nonlinear dielectric layer of dielectric function n_d^2 and thickness d. If an intense plane wave is incident on the structure of figure(1.1) from below, the refractive index of the nonlinear region changes. This change results in the reflectivity of the structure as experienced by the oblique wave to vary with the intensity of the lower wave. The effect of this change can be dramatic under conditions of resonant reflection. At a certain angle of incidence and under appropriate conditions, plasma-surface modes can be established on the metal surface resulting in the reduction of reflectivity to values that are close to zero. This situation is known as the surface plasmon resonance condition. Assuming that this condition is arrived at for a weak oblique signal, the existing conditions in this case are similar to those of the well-known Kretschmann configuration [2]. This resonance condition has been found to be extremely sensitive to the geometric and dielectric properties of the structure. In recent years its sensitivity has been used to measure the dielectric constants of metal films [3] and in organic overlayers [4]. More recently the surface-plasma mode resonance condition has been used in device realization. The early demonstrations using surface-plasma modes as optical gas detectors [5] and optical biosensors [6] and [7] have been receiving much renewed attention with a

view to improving the basic principle of operation [8]. In all the above applications of the surface-plasma mode resonance, only linear effects are involved. This M.S. thesis differs in nature from these applications because it relies on the existence of the nonlinear dielectric layer n_d of figure(1.1). Nonlinear operation is explained in the next section.

1.2 NONLINEAR REFLECTIVITY MODULATION

The basic mode of operation of the modulator of interest relies on the fact that the amplitude of a reflected beam from the structure shown in figure (1.1) at a particular angle depends on the refractive index of the layer adjacent to the lower surface of the metal. This means that if the refractive index of that layer is changed controllably, a beam of light incident from the prism can be modulated. Assuming this medium to be nonlinear, which means its refractive index depends on the intensity of the electric field existing in that layer, it is possible to change the reflectivity of the oblique wave of figure (1.1) by changing the intensity of the field present in the nonlinear layer.

It is seen that in order to modify the refractive index of the nonlinear dielectric n_d a second beam can be employed for this purpose. This is a

novel approach that has a new feature, namely the modulation of a beam of light by another beam. An experimental demonstration of this type of modulation has been reported recently by Moslehi, Foster and Harvey [9]. In this reference the active layer has been the photopolymer dyed polymethyl methacrylate. A red He-Ne beam has been used to excite the plasmon while a green beam has been used to modulate its index. It must be noted here that in the present work the beam incident from the prism is assumed to be weak and the changes in the refractive index of the nonlinear layer n_d is only due to the normally incident beam. Thus no nonlinear interaction takes place.

To account for the nonlinearity a numerical self-consistent approach is used. This approach is applied to the structure by assuming that the nonlinear region to be linear having the background dielectric constant and by subdividing the region into many layers. The electric field due to the beam incident from below is then calculated in each of the layers of the region. Once the electric field is calculated, it is allowed to modify the dielectric constant of the nonlinear region. This results in a graded index dielectric constant in the region under consideration. The electric field in the resulting graded index region is then calculated assuming the region to be linear. The procedure is repeated until a self-consistent field is obtained.

1.3 THESIS ORGANIZATION

This thesis consists of five chapters. The first chapter is an introductory chapter, which describes the optical structure of interest and states clearly the aim of the thesis. In addition, a short literature review is given. Chapter two, entitled surface plasmons and applications, discusses the surface plasmons and how to excite them. It also describes some applications of surface plasmons resonance. The numerical method used to account for the nonlinearity in our simulation will be presented in chapter three. Chapter four presents the results of this thesis while in chapter five future work and conclusions are presented.

Chapter two, on surface plasmons, consists of three sections, namely a general introduction to surface plasmons, surface plasmon excitation and applications of surface plasmon resonances. In the first section the important terms are defined and the derivation of the propagation constant of the surface plasmons are obtained. Prism coupling by using Kretschmann's configuration and Otto's configuration as well as grating coupling is presented in the second section. Three examples of the surface plasmon resonance applications are given in the third section.

These examples are spatial light modulators using surface plasmon resonance (SPR), surface plasmon microscopy and optical chemical sensing using SPR.

The wave equations of TE and TM polarizations are given in section two of chapter three. A separate section is devoted to the derivation of the amplitude reflection coefficient of a multilayer structure for both TE and TM polarized plane waves . The fourth section of chapter three discusses the numerical approach used in this thesis i.e. the self-consistent method. The validity of the self-consistent method in linear and nonlinear structures is presented in that section.

Chapter four presents the results of this thesis and it consists of four sections. In the first section all parameters used in this thesis and shown in figure (1.1) are discussed. In section two of the same chapter angle scanning and resonance curves are dealt with. The dependence of the reflectivity of the upper beam on the intensity of the normally incident beam is investigated. Finally, the effect of saturation on the level of modulation is investigated.

Chapter five reviews the results and gives some possible future work on the configuration shown in figure (1.1).

CHAPTER 2

SURFACE PLASMONS

2.1 GENERAL INTRODUCTION ON SURFACE PLASMONS

Consider a structure consisting of two semi-infinite media one of which is a non-conducting material with dielectric constant ε_d and the other a metal having a dielectric constant ε_m with negative real part, see figure (2.1). Such a structure can support a type of guided modes, where the power flows only along the interface between the two media and decays evanescently in both media. Such a mode is known as surface plasmons [10]. Surface plasmons exist only for TM (transverse magnetic) polarized electromagnetic waves. The restriction to the TM waves only comes from the fact that the field supported by this structure

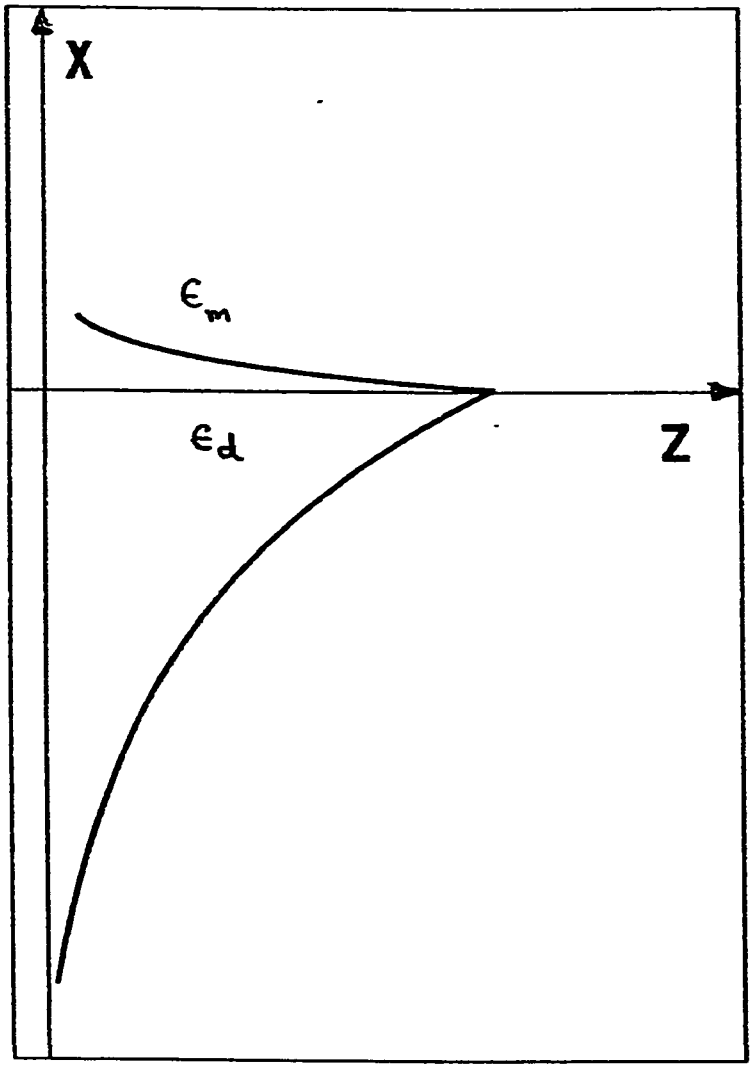

Figure (2.1) Diagram showing the interface between the metallic region with dielectric constant ε_m $(x>0)$ and the dielectric region with dielectric constant ε_d $(x<0)$ and an sample surface plasmon wave.

undergoes a change in the sign of its slope. Assume that the field decays in the two media as $A\,e^{-px}$ for $x > 0$ and $B\,e^{qx}$ for $x < 0$. The boundary conditions for TE waves whose components are E_y, H_x and H_z require the continuity of E_y and H_z. Applying these boundary conditions, the following two equations result.

$$A = B$$

and

$$p = -q$$

For the field to decay in the two media both p and q must be positive which contradicts the previous equation. As a result surface plasmons cannot exist for TE polarized waves. Assume now the field is TM polarized. The boundary conditions in this case are the continuity of H_y and E_z. Where E_z is proportional to the derivative of H_y divided by ε. Upon applying these conditions, we obtain the following two equations.

$$A = B$$

and

$$A\,p = -\frac{\varepsilon_m}{\varepsilon_d}\,q\,B \qquad (2.1)$$

Equation (2.1) is satisfied if and only if the ratio $\frac{\varepsilon_m}{\varepsilon_d}$ is negative. If a surface plasmon propagates in the z-direction and its field components vary as $\exp[i(\beta z - \omega t)]$ then the propagation constant of this wave is given by [10]:

$$\beta = \left(\frac{\omega}{c}\right)\left[\frac{\varepsilon_d \varepsilon_m}{\varepsilon_d + \varepsilon_m}\right]^{1/2} \qquad (2.2)$$

Where c is the speed of light and ω is the angular frequency.

2.1.1 The Propagation Constant Of A Surface Plasmon

Consider a plane interface separating two semi-infinite media one of which is a dielectric and the other is a metal. Assume that the x-axis is chosen perpendicular to the interface, which is the plane x = 0, see figure (2.1). We are looking for plane-wave solutions of TM-polarized waves that satisfy Maxwell's equations in each medium and also satisfy the boundary conditions at the interface. All electric and magnetic field components are assumed to have the following spatial and temporal dependence: $e^{i(\bar{k}\cdot\bar{r} - \omega t)}$ Where $\bar{k}$ is the wave vector and $\bar{r}$ is the position vector. Maxwell's equations for either medium are, as given by [11]:

$$\nabla \cdot \overline{E} = 0 \tag{2.3}$$

$$\nabla \cdot \overline{H} = 0 \tag{2.4}$$

$$\nabla \times \overline{E} = -\mu_0 \frac{\partial \overline{H}}{\partial t} \tag{2.5}$$

$$\nabla \times \overline{H} = \varepsilon \frac{\partial \overline{E}}{\partial t} \tag{2.6}$$

where it is assumed that all media are nonmagnetic (i.e. $\mu = \mu_0$), an assumption that is maintained throughout this thesis. Using the space-time dependence indicated above, equations (2.3)-(2.6) reduced to [12]:

$$\overline{k} \cdot \overline{E} = 0 \tag{2.7}$$

$$\overline{k} \cdot \overline{H} = 0 \tag{2.8}$$

$$\overline{k} \times \overline{E} = (\omega \mu_0) \overline{H} \tag{2.9}$$

$$\overline{k} \times \overline{H} = -(\omega \varepsilon) \overline{E} \tag{2.10}$$

For TM polarized waves the magnetic field $\overline{H}$ has no component in the direction of propagation which is taken to be the z-direction. By

choosing the y-axis parallel to $\overline{H}$ we have

$$H_x = 0 \quad , \quad H_z = 0 \quad , \quad H_y \neq 0$$

and from equation (2.8) we have the following relation:

$$k_y H_y = 0$$

hence,

$$k_y = 0$$

Taking the y-component of equation (2.10) we also have:

$$E_y = 0$$

The only non-vanishing field components are then H_y, E_x and E_z. These are the field components of a TM polarized wave. As a result, equation (2.7) reduces to:

$$k_x E_x + k_z E_z = 0 \qquad (2.11)$$

and equation (2.9) reduces to:

$$k_z E_x - k_x E_z = (\omega \mu_0) H_y \qquad (2.12)$$

while equation (2.10) results in the following relationships,

$$k_z H_y = (\omega \varepsilon) E_x \qquad (2.13)$$

$$k_x H_y = -(\omega \varepsilon) E_z \tag{2.14}$$

Equations (2.11)-(2.14) are not independent. In fact, equation (2.11) follows directly from (2.13) and (2.14). Upon substituting (2.12) into (2.13) and (2.14), we obtain a set of two homogeneous equations in E_x and E_z.

$$\left[\frac{1}{\omega \mu_0}\right] k_z (k_z E_x - k_x E_z) = (\omega \varepsilon) E_x \tag{2.15}$$

$$\left[\frac{1}{\omega \mu_0}\right] k_x (k_z E_x - k_x E_z) = -(\omega \varepsilon) E_z \tag{2.16}$$

Which gives:

$$\left[k_z^2 - \omega^2 \mu_0 \varepsilon\right] E_x - k_x k_z E_z = 0 \tag{2.17}$$

$$-k_x k_z E_x + \left[k_x^2 - \omega^2 \mu_0 \varepsilon\right] E_z = 0 \tag{2.18}$$

For these two equations to have a solution the determinant

$$\begin{vmatrix} k_z^2 - \omega^2 \mu_0 \varepsilon & -k_x k_z \\ -k_x k_z & k_x^2 - \omega^2 \mu_0 \varepsilon \end{vmatrix}$$

must vanish giving

$$k_x^2 + k_z^2 = \omega^2 \mu_0 \varepsilon \qquad (2.19)$$

Let us now consider the boundary conditions at the interface x=0, of figure (2.1). Since these must be satisfied for an arbitrary z, k_z must have the same values for both media. Therefore, equation (2.19), written out explicitly for the two media, becomes:

$$k_{xd}^2 + k_z^2 = \omega^2 \varepsilon_d \mu_0 \varepsilon_0 \qquad (2.20)$$

$$k_{xm}^2 + k_z^2 = \omega^2 \varepsilon_m \mu_0 \varepsilon_0 \qquad (2.21)$$

Equations (2.20) and (2.21) are two equations in three unknowns,namely k_{xm}, k_{xd} and k_z. A third equation can be found from the continuity of the field components at the interface. The components that are continuous are the tangential component of $\overline{E}$, namely E_z, the tangential component of $\overline{H}$, namely H_y and the normal component of $\overline{D}$ or εE_x.

The last two boundary conditions are in fact equivalent as can be seen from equation (2.14). Since k_z and E_z are both continuous, we conclude from equation (2.11) that the product $k_x E_x$ must also be continuous.

Thus:

$$k_{xd} E_{xd} = k_{xm} E_{xm} \tag{2.22}$$

The continuity of the normal component of $\overline{D}$ gives:

$$\varepsilon_d E_{xd} = \varepsilon_m E_{xm} \tag{2.23}$$

dividing equation (2.22) by equation (2.23) we obtain:

$$\frac{k_{xd}}{k_{xm}} = \frac{\varepsilon_d}{\varepsilon_m} \tag{2.24}$$

Now the three equations (2.20),(2.21) and (2.24) can be solved for three unknowns: k_{xd}, k_{xm}, k_z. The solution is given by [12]:

$$k_z = \left(\frac{\omega}{c}\right)\left[\frac{\varepsilon_d \varepsilon_m}{\varepsilon_d + \varepsilon_m}\right]^{1/2} \tag{2.25}$$

$$k_{xd} = \left(\frac{\omega}{c}\right)\frac{\varepsilon_d}{\left[\varepsilon_d + \varepsilon_m\right]^{1/2}} \tag{2.26}$$

$$k_{xm} = \left(\frac{\omega}{c}\right)\frac{\varepsilon_m}{\left[\varepsilon_d + \varepsilon_m\right]^{1/2}} \tag{2.27}$$

What concerns us most of these three equations is equation (2.25). That is because k_z is the wave-vector component along the axis of propagation.

In other words k_z is the propagation constant β which was given in equation (2.2).

2.2 SURFACE PLASMONS EXCITATION

Many of the important metals such as gold, silver and aluminum have dielectric constants with negative real parts at the optical and near-optical wavelength. Accordingly, the real part of $\varepsilon_m + \varepsilon_d$ is always smaller in magnitude than the real part of ε_m. This means that

$$\frac{\varepsilon_m}{\varepsilon_m + \varepsilon_d} > 1$$

$$\frac{\varepsilon_m \varepsilon_d}{\varepsilon_m + \varepsilon_d} > \varepsilon_d$$

$$\left(\frac{\omega}{c}\right)\left[\frac{\varepsilon_d \varepsilon_m}{\varepsilon_d + \varepsilon_m}\right]^{1/2} > \left(\frac{\omega}{c}\right)\sqrt{\varepsilon_d}$$

From the last relationship it is seen that β in equation (2.2) is always greater than $\omega\sqrt{\mu_0 \varepsilon_0 \varepsilon_d}$. As a consequence, light incident from the dielectric cannot couple to the plasmon waves and so a third coupling medium of refractive index $n_p > n_d$ is required. The refractive indices n_p and n_d are related to the dielectric constants by $n_p = \sqrt{\varepsilon_p}$ and

$n_d = \sqrt{\varepsilon_d}$. The purpose of the third medium is to slow down the incident light so that the phase matching condition is satisfied as will be explained later in the chapter.

2.2.1 Prism Coupling

There are two widely used methods of coupling incident light to the surface plasmon polariton. Both methods utilize prism coupling and are known as the Kretschmann configuration and the Otto configuration respectively. In this work the Kretschmann configuration, which is described below is used.

2.2.1.1 Kretschmann Configuration

Figure (2.2) shows the configuration which was proposed by Kretschmann in 1971 [2] to achieve coupling. It consists of a prism (ε_p) with a thin metallic film (ε_m) deposited on its base. A dielectric (ε_d) is assumed to constitute the substrate. When a TM polarized beam of wave-vector k is incident from the prism side, total internal reflection can occur at the base of the prism. This will generate an evanescent field extending through the metal film and a plasmon mode will be excited on the lower surface of the metal film. Figure (2.3) illustrates the resulting electric field intensity distributions at three different angles of incidence. Ray treatment of the three-medium structure is continuum. In other words, for any angle of incidence some of the incident beam is reflected to the prism and some is transmitted into the other two media. It is

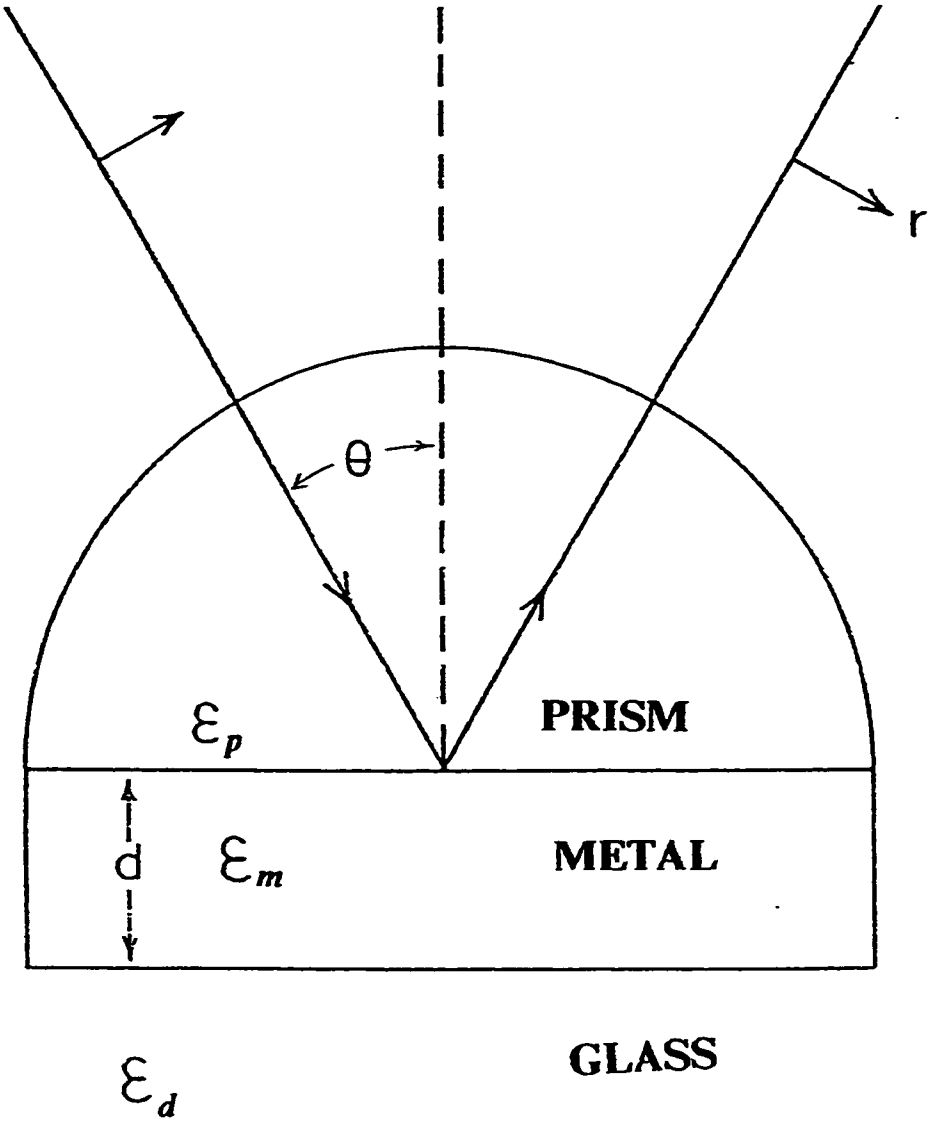

Figure (2.2) The configuration proposed by Kretschmann for prism coupling [12].

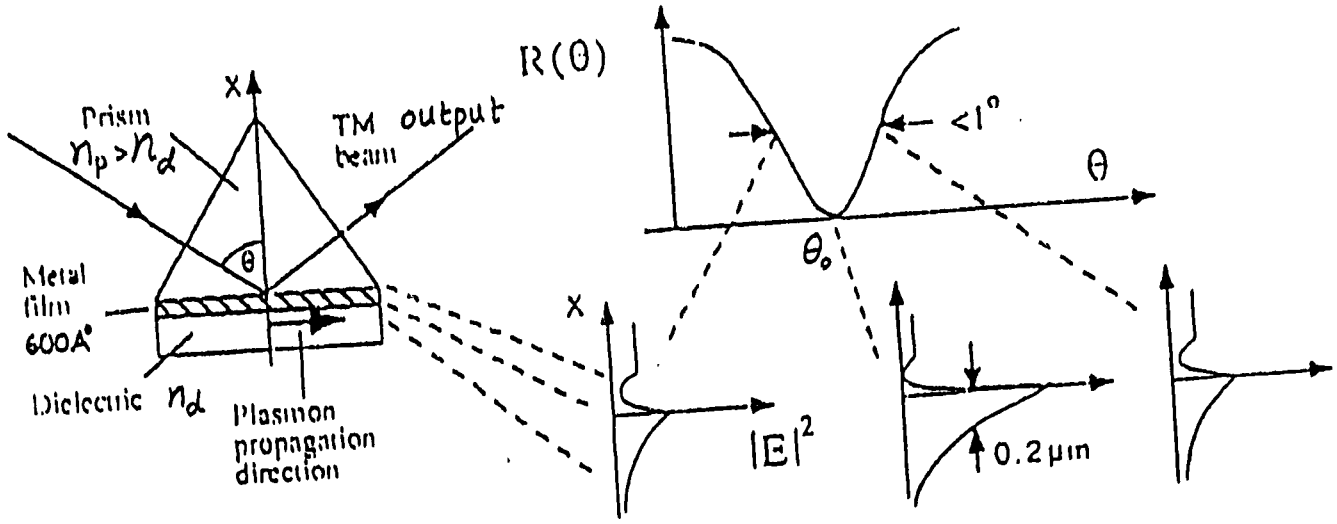

Figure (2.3) Illustrates the field intensity distribution of surface plasmon wave at three different angles of incidence [13].

clear from the figure that near the angle where phase matching is achieved the amplitude of the excited surface plasmon at the lower interface of the metal is in its most enhanced point while the amplitude of the reflected beam in the prism drops to its minimum [13]. By phase matching condition we mean, that the propagation constant of the surface plasmon $\beta \approx n_p k_0 \sin\theta$ where k_0 is the free space wave number given by $k_0 = \frac{\omega}{c}$. As a result of this the reflectivity will show a very sharp dip when phase matching condition is satisfied. This effect is known as surface plasmon resonance (SPR). A typical surface plasmon resonance curve is shown in figure (2.4).

For a resonant three-medium continuum mode the propagation constant can be defined as [13]:

$$\beta_3 = \beta_{3r} + i(\Gamma_i + \Gamma_r) \qquad (2.28)$$

Where β_{3r} is its real part and Γ_i and Γ_r represent the ohmic loss in the metal and is the radiative loss or leakage into the prism. Furthermore, the reflectivity curve or what is known as the SPR curve can be represented by [13]:

$$R(\theta) = 1 - \frac{4\Gamma_i \Gamma_r}{(n_p k_0 \sin\theta - \beta_{3r})^2 + (\Gamma_i + \Gamma_r)^2} \qquad (2.29)$$

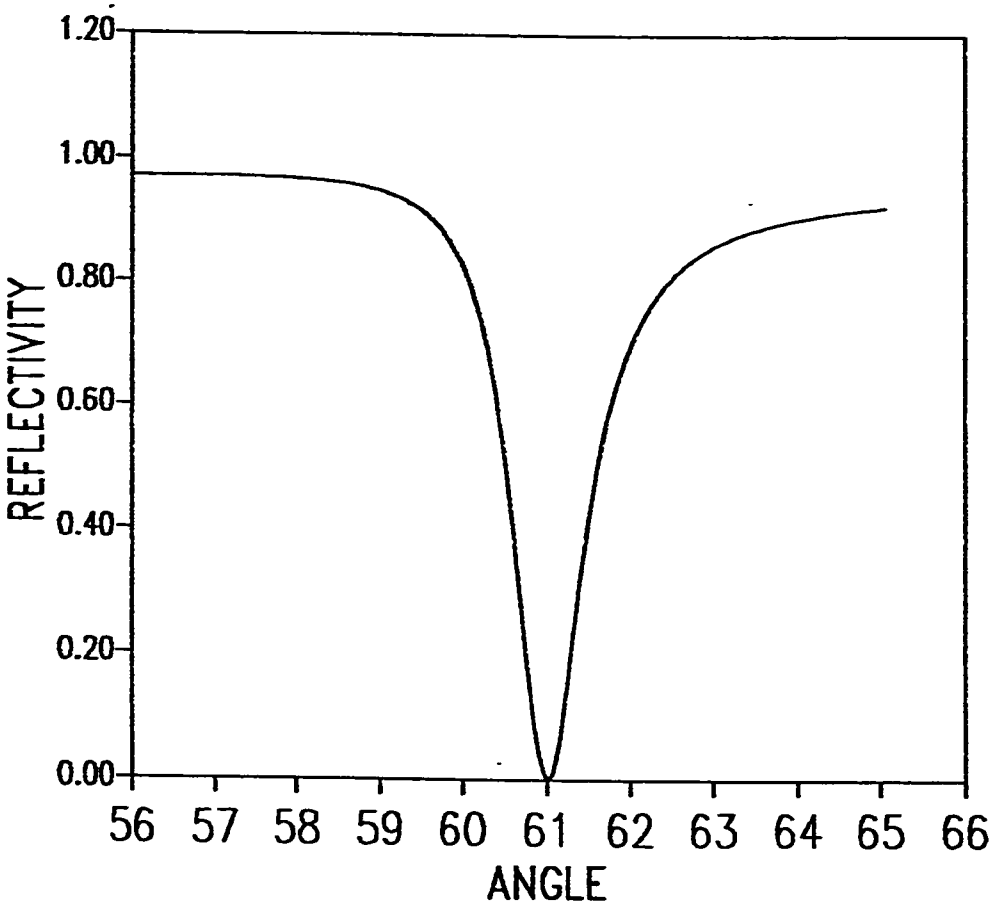

Figure (2.4) Typical surface plasmon resonance curve for configuration with prism, silver and air. The structure in figure (1.) was used.

Considering equation (2.29) it can be seen that an impedance matching condition is also required in order for the reflectivity to approach zero at resonance. This condition is given in equation (3.30).

$$\Gamma_i = \Gamma_r \tag{2.30}$$

This means at resonance all the incident beam is absorbed into the excited surface plasmon and the coupling efficiency of the structure is maximum. Impedance matching can be achieved by controlling the metal layer thickness [10].

In order to obtain large enhancement of the surface plasmon field at resonance, a metal having very high conductivity at optical frequency is required. This will result in a small Γ_i which gives a sharp reflectivity dip. At a wavelength of 633 nm silver is the most widely used metal and it satisfies equation (2.30) for a thickness near 560 Å [10]. These values give about 0.2° angular width and the amplitude of the plasmon at the lower interface of the metal is twice that of the incident beam [10]. The evanescent field extends about 0.2 μm into the dielectric in this case [10]. Gold also results in a good SPR curves at wavelength near infra-red [10].

2.2.1.2 Otto Configuration

Another prism coupling configuration was introduced by Otto in 1968. Figure (2.5) shows this configuration. It consists of a prism with a dielectric constant ε_p separated by an air gap from a thick metal or semiconductor sample that has a dielectric constant ε_m [14]. Under total internal reflection conditions there will always be an exponentially decaying evanescent field extending into the air gap. Also, the totally reflected wave has a component of wave number parallel to the surface equal to $n_p k_0 \sin\theta$. In this case the surface plasmon has a dispersion curve that lies below the air or vacuum light line ($\omega = c\,k_0$), but above the prism light line ($\omega = c\frac{k}{\sqrt{\varepsilon_p}}$) and the evanescent wave created by total reflection exists in the range $\theta_c < \theta < 90°$ or alternatively $\frac{1}{n_p} < \sin\theta < 1$. [12]

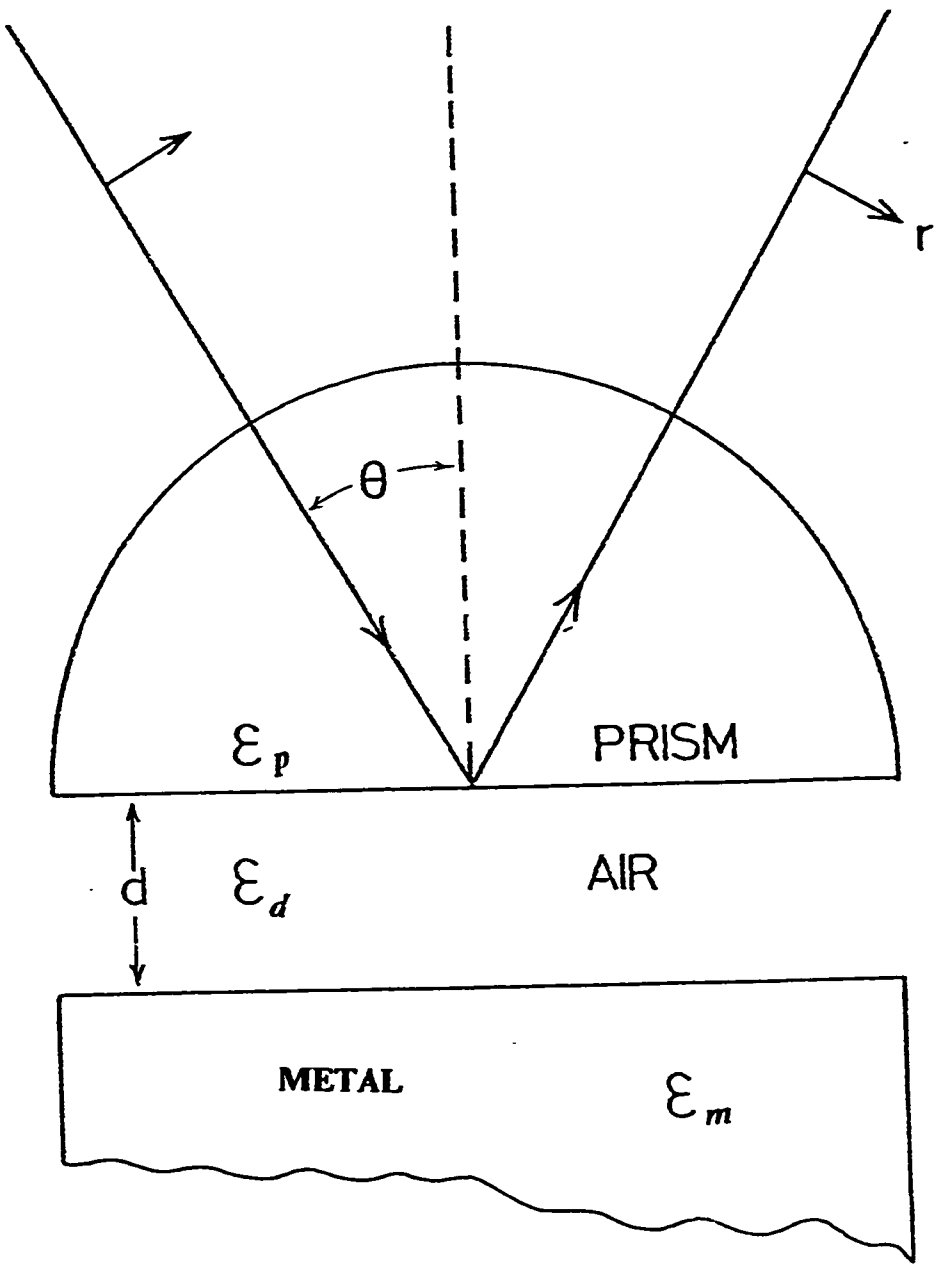

Figure (2.5) The configuration proposed by Otto for prism coupling [12].

2.2.2 Grating Coupling

For dielectrics with high ε_d, such as semiconductors, suitably high refractive index prisms cannot be obtained for prism coupling and instead grating couplers, which give similar SPR curves, are used. Dakss et al [15] reported the first coupling of a beam into a thin film by means of a dielectric grating. They used a thick photo-resist layer which was exposed to a 4800 Å laser interferometer fringe pattern and subsequently developed to yield a periodicity $d = 0.665\ \mu m$. A work by Kogelnik and Sosnowsky followed immediately that of Dakss [16]. They exposed a thick dichromated gelatin layer to a fringe pattern which was inclined at an angle of about 45° with respect to the surface of the layer. After these works many investigations followed which increased the understanding of grating couplers [17].

As can be seen from figure (2.6) grating couplers are equivalent to the prism couplers except that prism is replaced by the grating layer. This grating layer can be constructed by exposing a photo-resist film into a combination of two fields traveling opposite to each other [17]. The grating can have different shapes, such as sinusoidal, triangular and trapezoidal depending on the procedure used and the photo-resist film [18].

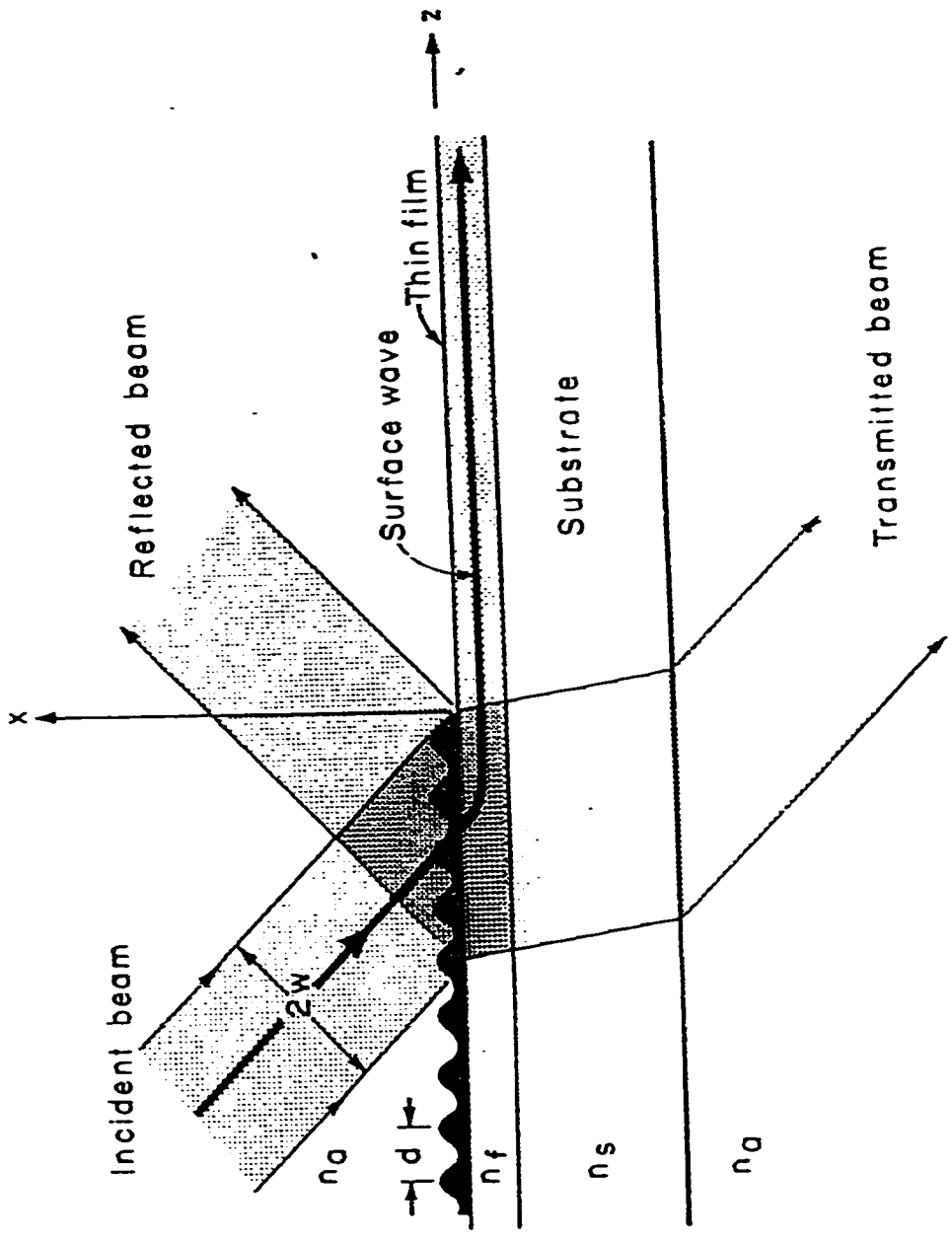

Figure (2.6) The schematic of a grating coupler [18].

In order for a thin film to support a surface plasmon using grating coupling, a phase matching condition must be achieved. This condition depends on the spaces between the harmonics in the grating. The propagation constant of these harmonics is defined as [17]:

$$\beta_v = \beta_0 + \left(2v\frac{\pi}{d}\right) \qquad v = 0, \pm 1, \pm 2, \ldots \qquad (2.31)$$

where β_0 is nearly equal to the surface-wave propagation constant β defined in equation (2.2) when the grating acts as small perturbation of the thin-film wave guide. But we know that for surface plasmons $\beta > k_a = \frac{2\pi}{\lambda_a}$, where λ_a is the wavelength in the superstrate. Which indicates that phase matching cannot be achieved unless v is a negative number, which is satisfied by equation (2.31). The following equation represents the phase matching condition.

$$k_a \sin\theta = \beta_v \qquad (2.32)$$

In order to achieve this matching condition suitable values of v, d, λ_a and θ must be chosen [17].

The main disadvantage of the grating couplers is that very large part of the incident light is often transmitted through the film and lost into the

substrate [17]. This is because grating couplers, unlike prism couplers do not work under total internal reflection. Another disadvantage is that if the ratio $\frac{d}{\lambda_a}$ is not small enough, energy can be lost into higher order diffracted beams produced by the grating [17]. This means grating cannot achieve easily the high efficiencies of the prism couplers. However their efficiency can be improved by just adding a small prism onto the grating couplers. This was shown by Dalgoutte [19]. He achieved an efficiency of about 70.5 percent.

2.3 APPLICATIONS OF SURFACE PLASMON RESONANCE

Although many applications of surface plasmon resonances have been developed, in this thesis only a few of them are described briefly. We will consider three types of devices which utilize surface plasmon resonance, namely spatial light modulators, surface plasmon microscopy and optical chemical sensors.

2.3.1 Spatial Light Modulator Utilizing SPR

Considering equation (2.2) we see that any changes in the refractive index of the layer below the metallic layer will result in shifting the resonance angle (angle where the reflectivity is nearly zero). Hence, we can excite a surface plasmon with different propagation constant by changing the refractive index of that layer. As an example of this we make reference to figure (2.7) which shows the resonance curves for three different refractive indices in the substrate. This extreme sensitivity to any changes in the refractive index of the layer next to the metal is the main advantage of surface plasmon resonance. Using a layer of electro-optic material in the layer beneath the metal we can achieve such changes controlably [10].

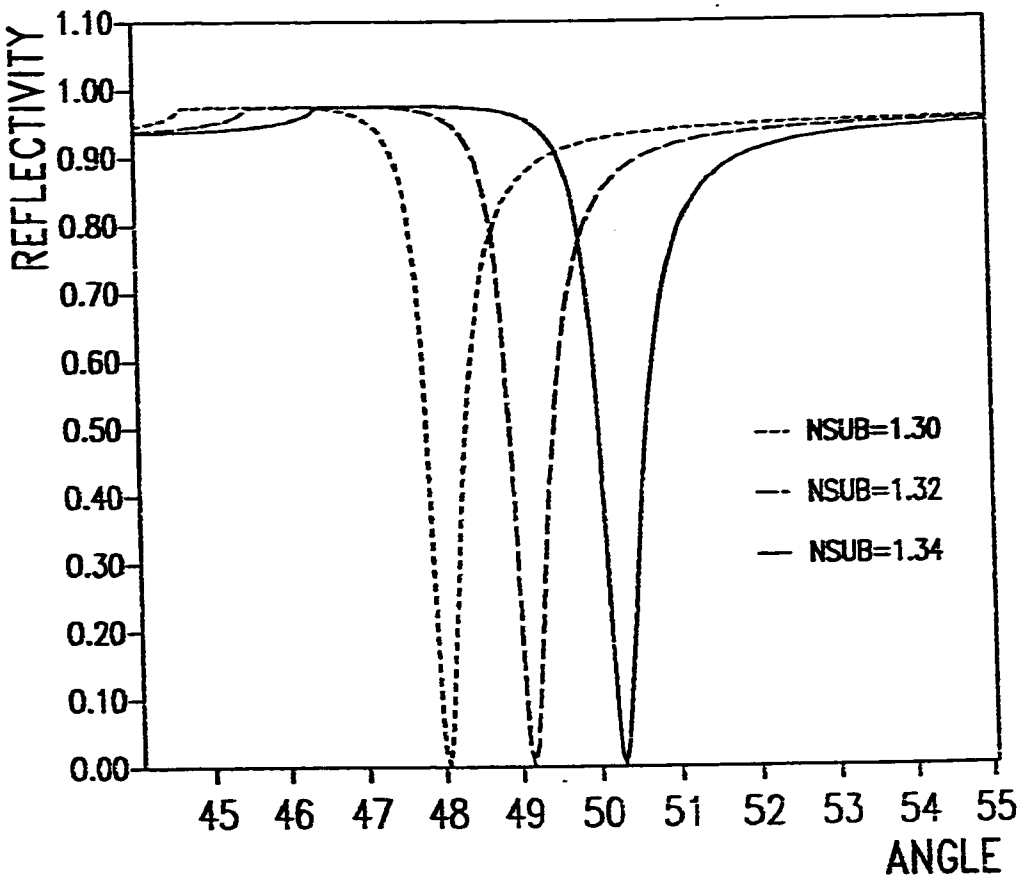

Figure (2.7) The resonance curves for three different refractive indexes in the substrate: 1.34, 1.32 and 1.30. The structure consists of prism metal and substrate of the given values.

Yeatman and Caldwell [10] [13] demonstrated a spatial light modulator that utilizes this change in the resonance angle. Their configuration is shown in figure (2.8). It contains a prism under which a thin metallic layer is deposited. Next a layer of electro-optic material (having a dielectric constant that changes with the electric field existing in that layer) is present. In order to produce the electric field that will change the dielectric constant of the electro-optic layer they put a strip column of metal under the electro-optic layer. These strips were connected to voltage sources as shown in the figure. Assuming a light is incident from the prism at a given angle, it will be reflected by the metal. However, if any voltage is present between any of the electrodes the dielectric constant above that electrode is changed resulting in shifting the resonance angle and changing the amount of the field reflected.

2.3.2 Surface Plasmon Microscopy

The imaging of low contrast samples is a challenging task for optical measuring techniques, especially if high lateral resolution is also required [20]. A new microscopy technique that uses surface plasmon polariton fields instead of normal light as the source of the illumination is called surface plasmon microscopy SPM. This technique offers a superior

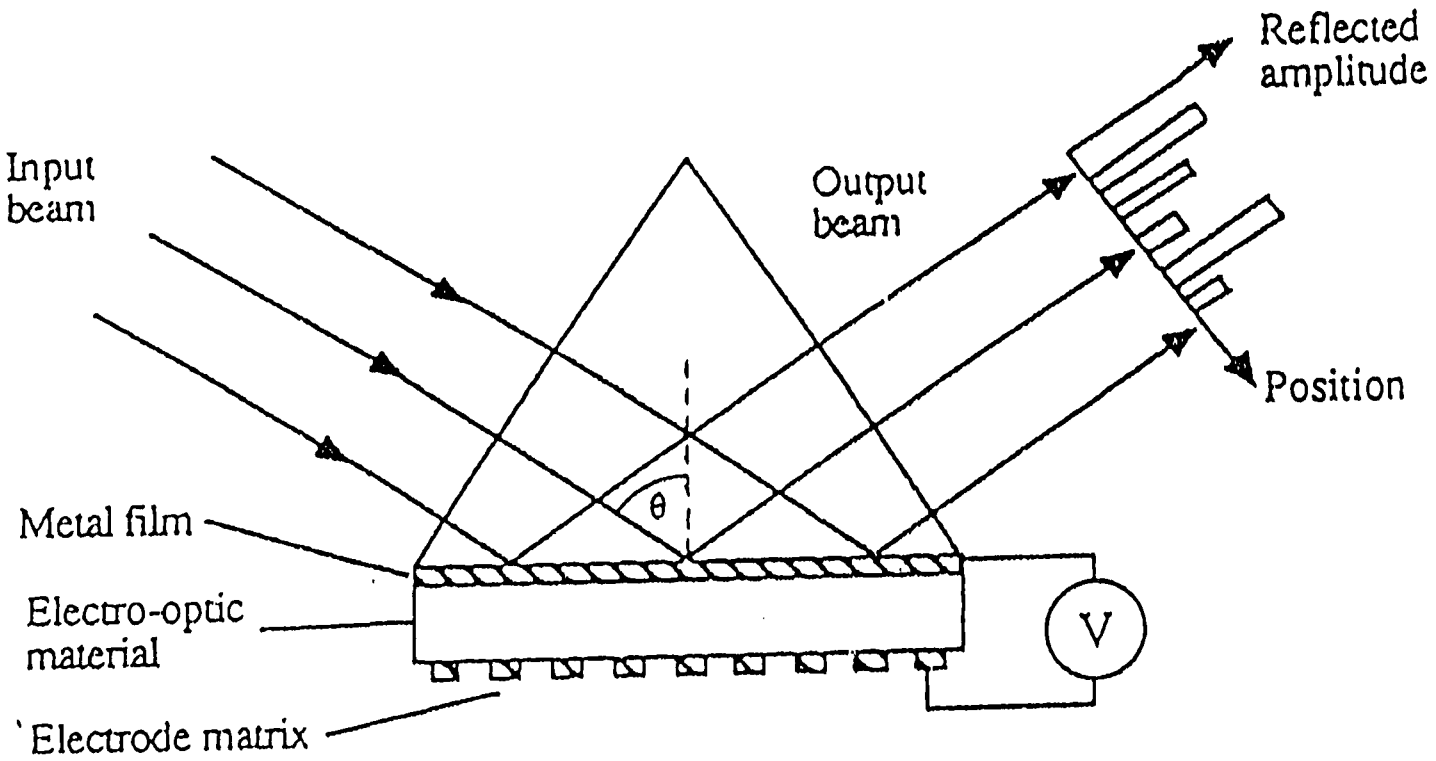

Figure (2.8) The spatial light modulator [10] and [13].

contrast without any loss of spatial resolution [20]. It makes use of the fact that surface plasmons are field having an enhanced amplitude at the interface supporting them when the resonance condition is achieved as discussed earlier in section 2.2.1.1.

The schematic set-up of the SPM is shown in figure (2.9). It consists of a prism under which a silver layer is present. The silver is coated from below by a thin dielectric layer. We know from the preceding sections that the surface plasmon wave will be excited if the resonance condition is achieved. But this condition depends on the layers present in the configuration: the prism, the metal, the coating dielectric and the substrate (air). Assume a light beam is incident into the prism and is exciting a surface plasmon on the surface between the metal and the dielectric layer. This means that the reflectivity at this angle is nearly zero. Now if any particles are present in the substrate the resonance angle will change from the previous one (the case of air only in the substrate), thus resulting in a very clear change in the reflectivity. All this is illustrated in figure (2.9). As an example of surface plasmon microscopy we can mention the experiment held by Rothenhausler and Knoll, whose schematic diagram is shown in figure (2.10). For more information refer to reference [20].

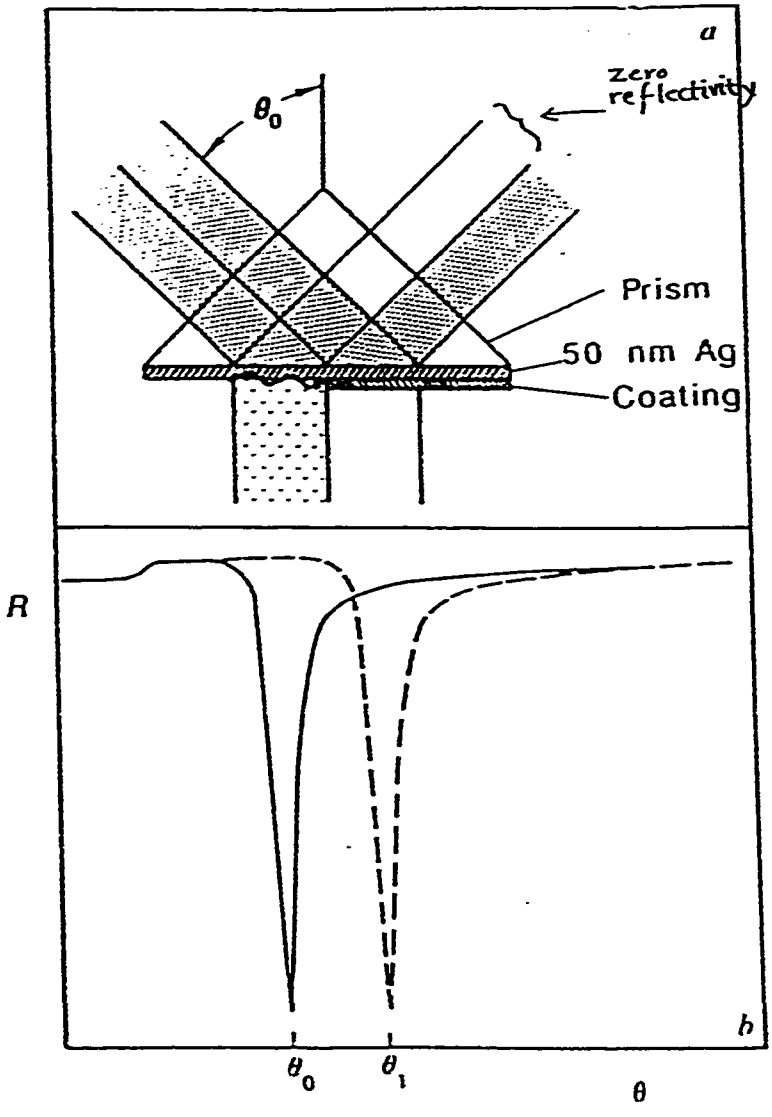

Figure (2.9) The basic principle of surface plasmon microscopy [19].

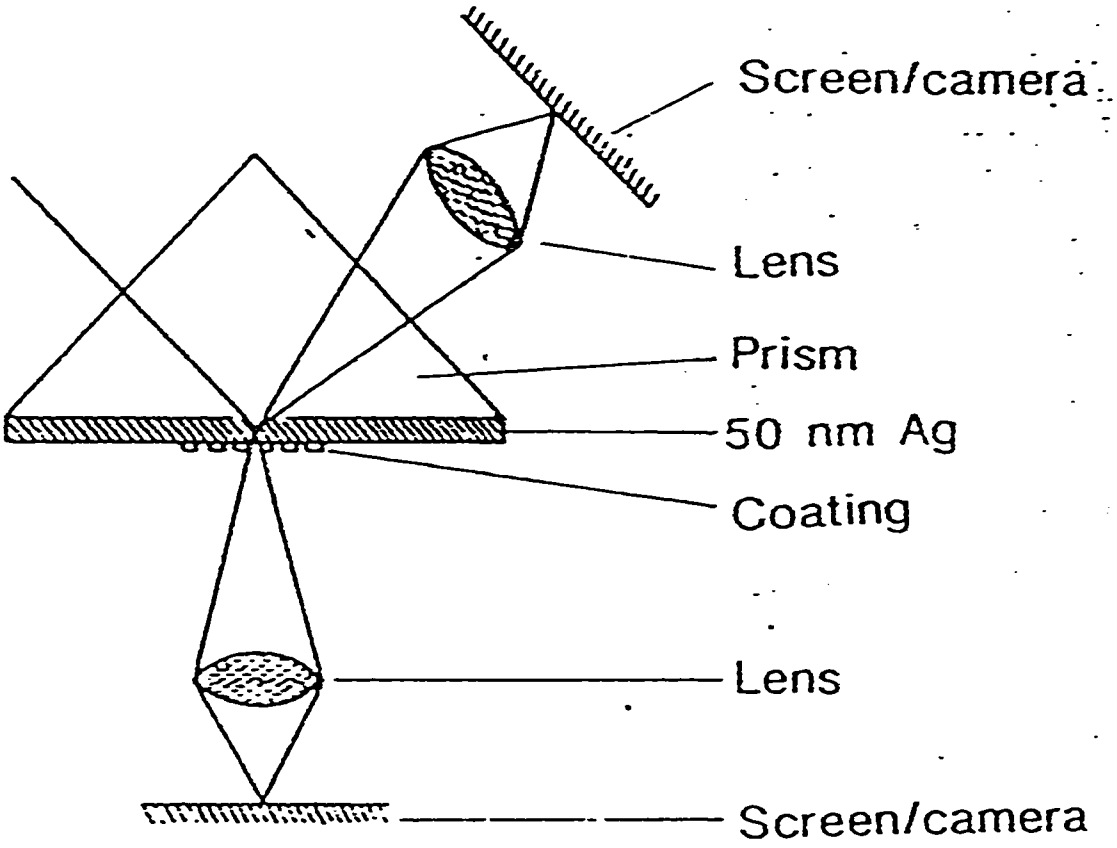

Figure (2.10) The schematic diagram of SPM [19].

2.3.3 Optical Chemical Sensing Using SPR

In recent years there have been a lot of interest in the measurement of liquid chemical concentrations by optical techniques [21]. This interest arises from the fact that optical techniques depend on light as a monitor of the concentration of the solution. This is so because in some applications electrical power used in sensors can be either inconvenient or hazardous while light is considered to be passive. In addition if fiber optics is used with the sensor that uses optical techniques, the system can be made compact and free from the effects of electromagnetic interference [21].

Zhang and Ultamchandani [22] reported a novel optical chemical sensor which utilizes surface plasmon resonance. Figure (2.11) shows the experimental configuration they used to implement the chemical concentration sensor. The configuration is composed of a prism under which a dielectric layer is present. A 60 nm thick silver film is deposited under the dielectric layer. The liquid solution of which the concentration is to be measured is kept in a small container as seen from the figure. If light is incident from the prism at a given angle, the reflected light is analysed by spectrum analyzer. Assuming the angle of incidence to be constant and its wavelength to be variable, a surface

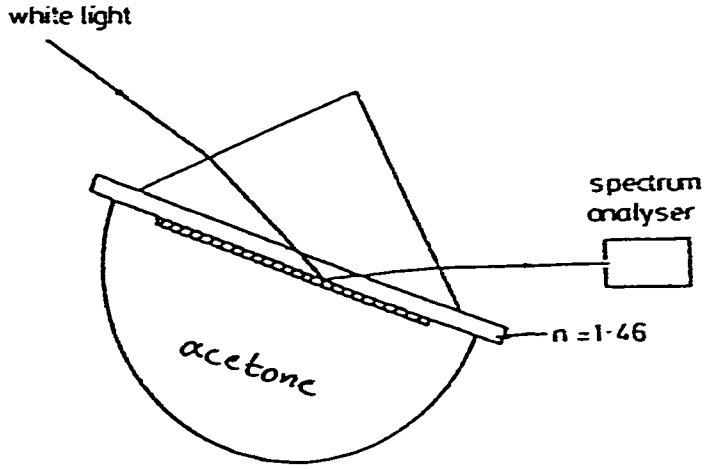

Figure (2.11) The optical chemical sensor based on SPR [21].

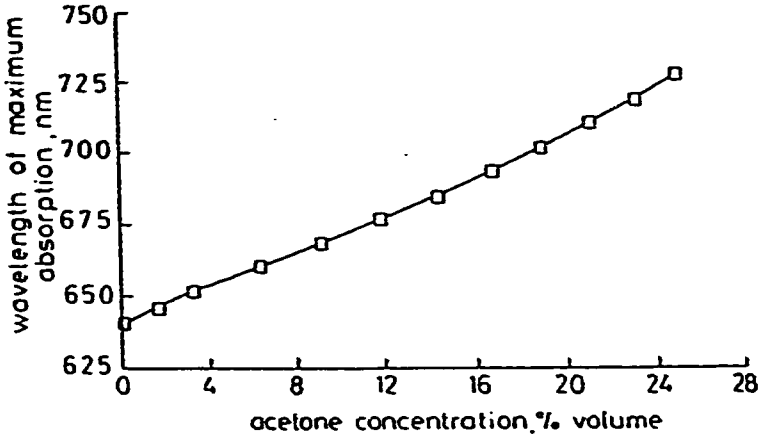

Figure (2.12) Illustrates the relation between concentration and the wave length of the maximum absorption [21].

plasmon will be excited at a specific wavelength for a given solution concentration. At this point almost all the incident light will be absorbed. This wavelength is referred to as the maximum absorption wavelength. As an example, if the solution is composed of acetone and water and its concentration varies from 0 to 25 % by volume, the dielectric constant will increase accordingly. The result of the experiment they conducted, given in figure (2.12) shows the maximum absorption wavelength changes from 640 nm at 0 % concentration to 727 nm at 25 % concentration [22]. This change is 87 nm which is very good indication of the concentration changes.

CHAPTER 3

THEORY AND METHOD OF CALCULATION

3.1 INTRODUCTION

This chapter is intended to give the general background required for the discussion of the problem investigated in this thesis and its possible solution. The chapter is divided into two main parts. In the first part Maxwell's equations are stated and starting from them the wave equation of TE (transverse electric) and TM (transverse magnetic) waves are derived. This is followed by a description of reflection from a multilayer structure. In the second part, the numerical multilayer method used in the calculations (the self-consistent method) is given in detail. In addition, the validity of the method in applications to linear and

nonlinear problems is discussed. finally, the validity of the method is tested for different intensities of incident light into the structure used.

3.2 MAXWELL EQUATIONS

James Clerk Maxwell is regarded as the founder of electromagnetic theory in its present form. As such Maxwell work led to the discovery electromagnetic waves. Although the laws of electromagnetism which Maxwell put together in the form of four equations were introduced in equations (2.3)-(2.6), we will present them in the next subsection in their most general form because of their importance to this chapter.

3.2.1 The Maxwell's Equations and Wave Equation

Maxwell's equations are:

$$\nabla \times \overline{E} = -\frac{\partial \overline{B}}{\partial t} \tag{3.1}$$

$$\nabla \times \overline{H} = \overline{J} + \frac{\partial \overline{D}}{\partial t} \tag{3.2}$$

$$\nabla \cdot \overline{B} = 0 \tag{3.3}$$

$$\nabla \cdot \overline{D} = \rho_v \qquad (3.4)$$

Where

$\overline{D}$ = electric flux density (Coulomb per meter square)

$\overline{E}$ = electric field strength (Volt per meter)

$\overline{B}$ = magnetic flux density (Weber per meter)

$\overline{H}$ = magnetic field strength (Ampere per meter)

These are vectors and they are functions of space and time. To show that they are vectors we used a bar over them. $\overline{J}$ is electric current density (Amp per Meter square) and ρ_v is electric charge density (Coulomb per Meter cube). These two equations are the sources generating the electromagnetic fields. Equations (3.1)-(3.4) express the physical laws governing the $\overline{E}, \overline{D}, \overline{H}$ and $\overline{B}$ fields and the sources $\overline{J}$ and ρ_v at every point in the space and at all times.

We concern ourself with source free regions and time-harmonic fields at a single frequency:

$$\rho_v = 0$$

$$\overline{J} = 0$$

$$\overline{B}(r,t) = \overline{B}(r)\, e^{-i\omega t}$$

and similarly for the other field equations $\overline{E}$, $\overline{D}$ and $\overline{H}$. The resulting Maxwell's equations are:

$$\nabla \times \overline{E} = i\omega\overline{B} \tag{3.5}$$

$$\nabla \times \overline{H} = -i\omega\overline{D} \tag{3.6}$$

$$\nabla \cdot \overline{B} = 0 \tag{3.7}$$

$$\nabla \cdot \overline{D} = 0 \tag{3.8}$$

From equations (3.5)-(3.8) it can be seen that there are 12 unknown components needed to be found from the Maxwell's equations. But Maxwell's equations give less than 12 scalar equations which means they are not sufficient to solve for the 12 unknowns. The six more scalar equations needed come from the constitutive relations. Physically, the constitutive relations provide information about the environment in which electromagnetic fields occur. Mathematically, we may characterize a simple medium with a permittivity ε and permeability μ as follows:

$$\overline{D} = \varepsilon \overline{E} \tag{3.9}$$

$$\overline{B} = \mu \overline{H} \tag{3.10}$$

As a result equations (3.5)-(3.8) become

$$\nabla \times \overline{E} = i\mu\omega\overline{H} \tag{3.11}$$

$$\nabla \times \overline{H} = -i\varepsilon\omega\overline{E} \tag{3.12}$$

$$\nabla \cdot \overline{H} = 0 \tag{3.13}$$

$$\nabla \cdot \overline{E} = 0 \tag{3.14}$$

Taking the curl of equation (3.11) we obtain

$$\nabla \times \nabla \times \overline{E} = i\mu\omega(\nabla \times \overline{H}) \tag{3.15}$$

and by using the mathematical identity

$$\nabla \times \nabla \times \overline{E} = \nabla(\nabla \cdot \overline{E}) - \nabla^2\overline{E} \tag{3.16}$$

together with equation (3.12) we obtain the wave equation for the electric field.

$$\nabla^2\overline{E} + \mu\varepsilon\omega^2\overline{E} = 0 \tag{3.17}$$

Where ∇^2 is the Laplacian operator and the wave number k is given by $k = \omega\sqrt{\mu\varepsilon}$. In a similar way the wave equation for the magnetic field is found to be,

$$\nabla^2 \overline{H} + \mu \varepsilon \omega^2 \overline{H} = 0 \qquad (3.18)$$

Writing the Laplacian operator ∇^2 in full equation (3.17) has the following form

$$\left[\frac{\partial^2}{\partial x^2} + \frac{\partial^2}{\partial y^2} + \frac{\partial^2}{\partial z^2} + k^2 \right] \overline{E} = 0 \qquad (3.19)$$

For the multilayer structure investigated in this thesis the media and the fields are assumed not to vary in the y-direction so that the term $\frac{\partial^2}{\partial y^2}$ in equation (3.19) vanishes. Accordingly, the resulting wave equation of interest in this research is,

$$\left[\frac{\partial^2}{\partial x^2} + \frac{\partial^2}{\partial z^2} + k^2 \right] \overline{E} = 0 \qquad (3.20)$$

The x-direction is now chosen to be normal to all interfaces of the multilayer structure, shown in figure (3.1). Solution of equation (3.20) in each layer of the figure is assumed to have the form $\exp\{ -i (\omega t - \beta z) \}$. Accordingly $\frac{\partial \overline{E}}{\partial z}$ is equal to $i \beta \overline{E}$ and equation (3.20) reduces to:

$$\left[\frac{\partial^2}{\partial x^2} + k^2 - \beta^2\right]\overline{E} = 0 \qquad (3.21)$$

A similar equation is obtained for the magnetic field strength $\overline{H}$ as follows:

$$\left[\frac{\partial^2}{\partial x^2} + k^2 - \beta^2\right]\overline{H} = 0 \qquad (3.22)$$

3.2.2 Field Components of TE and TM waves

Because the fields that exist in a planar waveguide are either of the TE type or of the TM type, the corresponding relationships between the field components of these two types are stated in the next subsection.

3.2.2.1 Wave equation for TE waves

In the previous section the z-axis has been chosen to be the direction of propagation while no variation is assumed to take place along the y-axis. In addition, TE waves are characterized by a single electric component E_y and two components of the magnetic field: H_x and H_z. If a substitution of the single electric field component is made into equation (3.21), we obtain:

$$\left[\frac{\partial^2}{\partial x^2} + k^2 - \beta^2\right] E_y = 0 \qquad (3.23)$$

Which can be easily solved. The two magnetic field component are calculated from equation (3.12) as follows:

$$H_x = \frac{i}{\mu\,\omega}\,\frac{\partial E_y}{\partial z} \qquad (3.24)$$

and

$$H_z = \frac{-i}{\mu\,\omega}\frac{\partial E_y}{\partial x} \tag{3.25}$$

Equation (3.24) reduces to the following equation.

$$H_x = -\frac{\beta}{\mu\,\omega}E_y \tag{3.26}$$

3.2.2.2 Wave equation for TM waves

For this type of polarization the only nonzero field components are H_y, E_x and E_z. In a similar procedure to that of the TE case the wave equation of the TM waves is written in terms of H_y as.

$$\left[\frac{\partial^2}{\partial x^2} + k^2 - \beta^2\right]H_y = 0 \tag{3.27}$$

The relationship between H_y and E_x and E_z can be found from (3.11) as,

$$E_x = \frac{\beta}{\varepsilon\,\omega}H_y \tag{3.28}$$

$$E_z = \frac{i}{\varepsilon \omega} \frac{\partial H_y}{\partial x} \tag{3.29}$$

3.3 REFLECTION FROM MULTILAYER REGIONS

The multilayer structure which is used in this thesis is shown in figure (3.1). It is composed of a semi-infinite superstrate or the medium of incidence with refractive index n_p , a semi-infinite substrate which is the medium of transmission with refractive index n_h and N number of layers in between each having refractive index n_l. The superstrate occupies the region $x < 0$ while the other media occupy the region $x > 0$. The position of the far end of layer l is designated P_l. The analysis in this section will be divided into two subsections: the first is devoted to TE waves and the second to TM waves.

3.3.1 TE - Polarized Waves

Equation (3.23) can be written for each of the different layers of the multilayer structure as:

Superstrate:
$$\left[\frac{\partial^2}{\partial x^2} + q_p^2\right] E_y = 0 \tag{3.30}$$

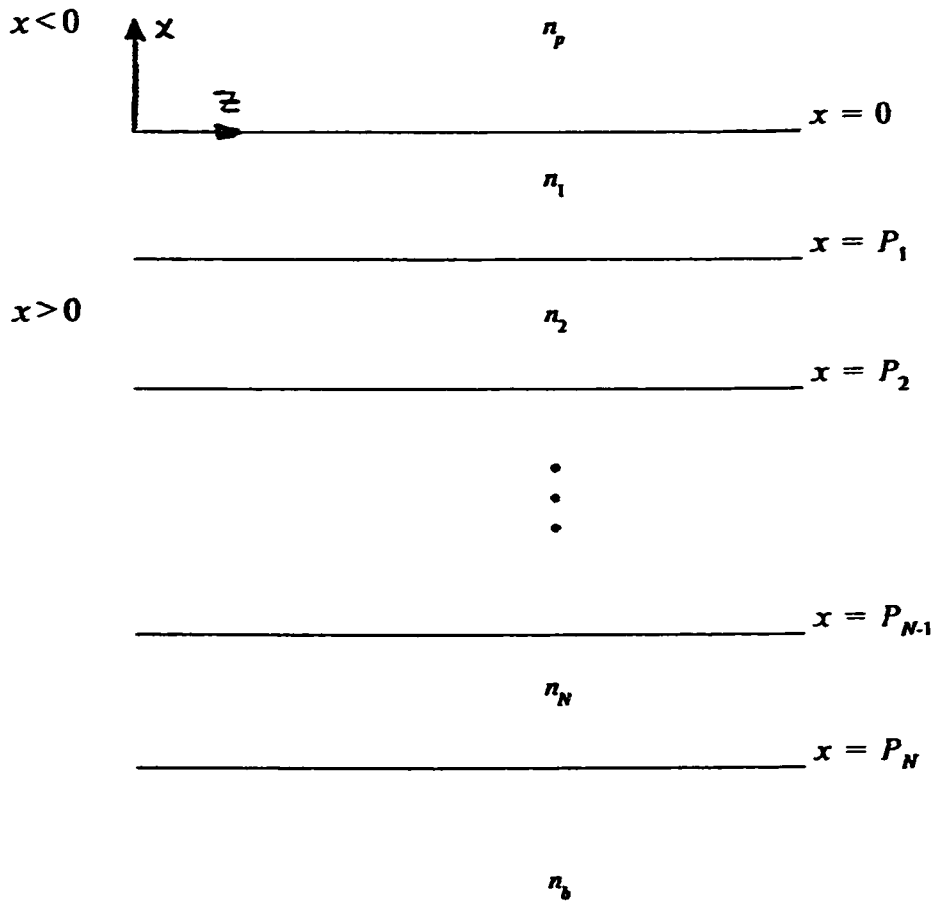

Figure (3.1) The system under investigation in this thesis. It comprises N layers materials bounded by two semi-infinite regions.

For Layers 1 to N: $$\left[\frac{\partial^2}{\partial x^2} + q_l^2\right]E_y = 0 \qquad (3.31)$$

and

Substrate: $$\left[\frac{\partial^2}{\partial x^2} + q_b^2\right]E_y = 0 \qquad (3.32)$$

Where $$q_p^2 = n_p^2 k_0^2 - \beta^2 \qquad (3.33)$$

$$q_l^2 = n_l^2 k_0^2 - \beta^2 \qquad (3.34)$$

$$q_b^2 = n_b^2 k_0^2 - \beta^2 \qquad (3.35)$$

The solution of equations (3.30) - (3.32) is given below and also shown in figure (3.2)

$$E_y = \begin{cases} A_p e^{iq_p x} + R A_p e^{-iq_p x} & x < 0 \\ A_l \cos q_l(x - P_l) + B_l \sin q_l(x - P_l) & P_{l-1} < x < P_l \\ A_b e^{iq_b(x - P_N)} & x > P_N \end{cases} \qquad (3.36)$$

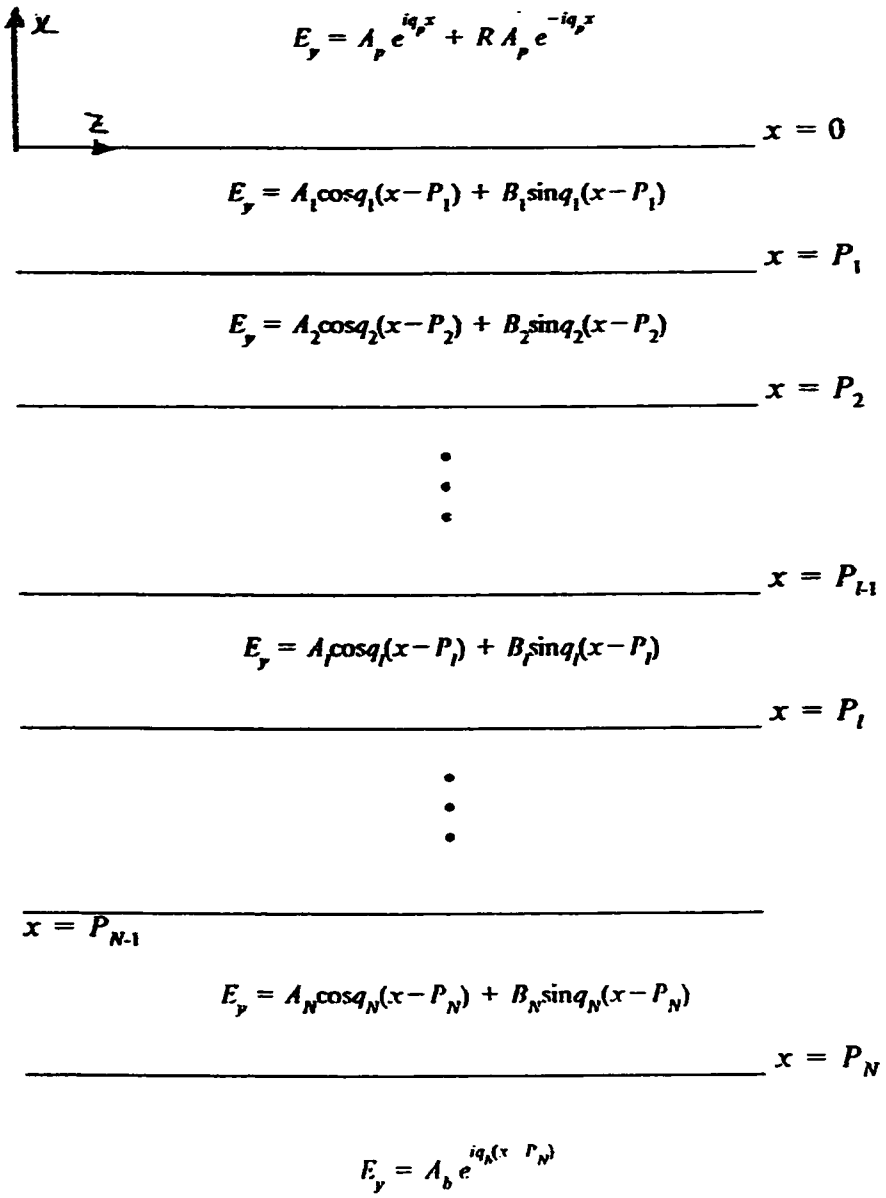

Figure (3.2) Figure illustrating the general electric field distribution in each layer of the multilayer structure used in this thesis.

where R is the amplitude reflection coefficient. Clearly the superstrate is the region where an incoming and outcoming solutions are assumed to coexist. These correspond to the incident and reflected waves. The substrate is seen to accommodate an outgoing solution only corresponding to the transmitted wave.

It is seen from equation (3.36) that there are two unknown amplitude coefficients A_l and B_l in each of the regions l = 1 ... N. Thus, we have a total of (2N+3) unknowns. To solve for these unknowns the boundary conditions must be applied. It has been stated earlier that a TE wave has E_y, H_x and H_z as its field components. Boundary conditions require that E_y and H_z must be continuous at each interface of the multilayer structure. Thus the (N+1) boundaries present in the multilayer structure will give (2N+2) equations. To solve these equations we assume one of the amplitude coefficients to be equal to unity and arrange the equations in a matrix form with the unknowns forming (2N+2) column matrix and the coefficients forming a (2N+2) square matrix. The solution is then obtained by inverting the square matrix. This procedure is straightforward but tedious. This method of solution is not followed in this work, rather a recursive solution which is more suited to computer programing is followed.

For completeness of description the field component H_z is found from equation (3.25) to be, as :

$$H_z = \left(\frac{-i}{\omega \mu}\right) \begin{cases} i q_p A_p e^{iq_p x} - i q_p R A_p e^{-iq_p x} & x<0 \\ -q_l A_l \sin q_l(x-P_l) + q_l B_l \cos q_l(x-P_l) & P_{l-1}<x<P_l \\ iq_b A_b e^{iq_b(x-P_N)} & x>P_N \end{cases} \tag{3.37}$$

Assuming A_b to be equal to unity the boundary conditions on E_y and H_z applied at interface N, give the following two equations:

$$A_N = 1 \tag{3.38}$$

and

$$B_N = \frac{i q_b}{q_N} \tag{3.39}$$

In order to make use of equations (3.38) and (3.39) in a recursive scheme the relationship between A_N and B_N on one hand and A_{N-1} and B_{N-1} on the other must be established. Clearly the recursive scheme thus, enables the amplitudes A_{l-1} and B_{l-1} of the $(l\text{-}1)^{th}$ layer to be obtained in terms of those of the l^{th} layer as follows,

$$A_{l-1} = A_l \cos q_l (P_l - P_{l-1}) - B_l \sin q_l (P_l - P_{l-1}) \tag{3.40}$$

and

$$B_{l-1} = \frac{q_l}{q_{l-1}} \left[A_l \sin q_l (P_l - P_{l-1}) + B_l \cos q_l (P_l - P_{l-1}) \right] \tag{3.41}$$

The boundary conditions at x=0 result in:

$$(1 + R) A_p = A_1 \cos q_1 P_1 - B_1 \sin q_1 P_1 \tag{3.42}$$

and

$$(1 - R) A_p = \frac{q_1}{i q_p} \{ A_1 \sin q_1 P_1 + B_1 \cos q_1 P_1 \} \tag{3.43}$$

dividing equation (3.43) by (3.42) we obtain:

$$\frac{1 - R}{1 + R} = \left[\frac{q_1}{i q_p} \right] \frac{A_1 \sin q_1 P_1 + B_1 \cos q_1 P_1}{A_1 \cos q_1 P_1 - B_1 \sin q_1 P_1} \tag{3.44}$$

Let us now define the following:

$$\gamma^{TE} = \frac{1 - R^{TE}}{1 + R^{TE}} \tag{3.45}$$

Which results in an amplitude reflection coefficient given by

$$R^{TE} = \frac{1 - \gamma^{TE}}{1 + \gamma^{TE}} \tag{3.46}$$

Finally, A_p can be found from equation (3.40) or (3.41). It is noted that a value of A_b other than unity will modify the amplitude coefficients A_t and B_t by a simple ratio between the the desired amplitude and the calculated amplitude. However, this will not change the profile of the field.

3.3.2 TM - Polarized Waves

For this polarization, as was stated earlier, the nonzero field components are H_y, E_x, and E_z. Solutions of the wave equation in the three regions of figure (3.1) is obtained in terms of H_y. In this case H_y replaces E_y in equations (3.30) - (3.32). The solution is written as follows

$$H_y = \begin{cases} A_p e^{iq_p x} + R A_p e^{-iq_p x} & x<0 \\ A_l \cos q_l(x-P_l) + B_l \sin q_l(x-P_l) & P_{l-1}<x<P_l \\ A_b e^{iq_b(x-P_N)} & x>P_N \end{cases} \tag{3.47}$$

and from equation (3.29) the component E_z is found to be,

$$E_z = \left(\frac{i}{\omega \varepsilon_0}\right) \begin{cases} \frac{i q_p}{\varepsilon_p}\left(A_p e^{iq_p x} - R A_p e^{-iq_p x}\right) & x<0 \\ \frac{q_l}{\varepsilon_l}\left(-A_l \sin q_l(x-P_l) + B_l \cos q_l(x-P_l)\right) & P_{l-1}<x<P_l \\ \frac{i q_b}{\varepsilon_p} A_b e^{iq_b(x-P_N)} & x>P_N \end{cases} \tag{3.48}$$

As in the TE case of previous section A_b is taken to be unity while the boundary conditions at $x = P_N$ gives:

$$A_N = 1$$

and

$$B_N = \frac{i\,q_b}{q_N}\left[\frac{\varepsilon_N}{\varepsilon_b}\right] \tag{3.49}$$

It is instructive to note that in the expression of B_N above, the ratio of the dielectric constants of the two adjacent media occur as a multiplicative parameter. This parameter is missing for TE polarized waves and underlies the difference in the behavior of the two types of polarization. In a manner similar to that used for TE waves in the previous section the recursive relationship of the amplitude coefficients is found to be,

$$A_{l-1} = A_l \cos q_l (P_l - P_{l-1}) - B_l \sin q_l (P_l - P_{l-1}) \tag{3.50}$$

and

$$B_{l-1} = \left[\frac{\varepsilon_{l-1}\, q_l}{\varepsilon_l\, q_{l-1}}\right] \{A_l \sin q_l (P_l - P_{l-1}) + B_l \cos q_l (P_l - P_{l-1})\} \tag{3.51}$$

Application of the boundary conditions at interface x=0 results in two equations in A_p and R which can then be solved to give A_p and R. These two equations are:

$$(1 + R)\, A_p = A_1 \cos q_1\, P_1 - B_1 \sin q_1\, P_1 \tag{3.52}$$

and

$$(1 - R)\, A_p = \frac{q_1}{i\, q_p}\left[\frac{\varepsilon_{l+1}}{\varepsilon_l}\right]\{A_1 \sin q_1\, P_1 \; + \; B_1 \cos q_1\, P_1\} \qquad (3.53)$$

Dividing equation (3.53) by equation (3.52) and defining

$$\gamma^{TM} = \frac{1 - R^{TM}}{1 + R^{TM}} \qquad (3.54)$$

the amplitude reflection coefficient is given by:

$$R^{TM} = \frac{1 - \gamma^{TM}}{1 + \gamma^{TM}} \qquad (3.55)$$

And A_p can be found from equation (3.52).

3.4 THE SELF-CONSISTENT APPROACH

3.4.1 Introduction

The self-consistent approach is a numerical technique that transforms a nonlinear problem into successive linear problems. It has been introduced by Dios and others in 1989 [24] to solve the TE wave equation of a planar structure that contains a nonlinear medium. In this thesis we will use this method with TM waves in order to account for the nonlinearity existing in our structure shown in figure (1.1). Although the structure shows two beams, only the normal beam is considered to affect the nonlinear medium. This assumption is made because physical nonlinearities are always weak. The normal beam is therefor much more intense than the oblique beam. In order to apply the self-consistent approach, we divide the nonlinear medium into very small layers in each of which the dielectric constant is assumed to be homogenous. Then starting with weak beams, linear theory can be used to obtain the field in the four regions of figure (1.1) with the refractive index of the nonlinear layer simply being the background refractive index. The field calculated is then used to modify locally the refractive index of the nonlinear region producing a graded index distribution within it. Linear theory is applied

once again to obtain the field in the modified structure. The procedure is repeated until a self-consistent field is arrived at. Normally, eight to nine iterations are needed to produce a self-consistent field with the number of layers being approximately two hundred.

To start with, the implementation of the equations given in the preceding section is made in order to show that the results given by this method are equivalent to those produced from analytical formulas. A three-layer structure was chosen for this purpose. The validity of the program at three different intensities is tested. For very low incident field intensities the nonlinearity of the active region can be neglected. The analytical expression for the reflectivity gives accurate description and it is possible to verify our approach by comparison with the analytical formula. Similarly linear theory hold for very high incident field intensities since in this case the nonlinear region becomes fully saturated. For intermediate field intensities linear theory is not applicable and the verification is done by comparison with another nonlinear approach as will be explained in section (3.4.3.2).

3.4.2 The Self-Consistent Approach Implementation

The program used in this thesis finds the reflectivity of a given structure provided its layers are linear . In addition to that, it finds the field distribution in all layers. In order to use the program with our structure, which contains a nonlinear medium, we divided the nonlinear medium into N-1 layers where the refractive index of each layer in the nonlinear medium is modified by the local field and reviewed several times until self-consistence is achieved .

In what follows, the theory of the computer program is given. To start with, the program reads the angle of incidence of the plane wave 0 and the magnetic field intensity H_{Dy}^2, at the metal-superstrate interface. Using these two values and the parameters provided about the structure, the program calculates n_e the effective refractive index given by:

$$n_e = n_p \sin 0$$

The program is then provided by the total number of layers of the nonlinear medium plus the metallic medium N. The program gives the background dielectric constant to each layer in the nonlinear region and calculates the parameters q_p , q_l and q_h required in equations (3.50) through (3.53) using the following,

$$q_p = k_0 \sqrt{n_p^2 - n_e^2}$$

$$q_l = k_0 \sqrt{n^2_l - n^2_e}$$

and

$$q_b = k_0 \sqrt{n^2_b - n^2_e}$$

At this point, the program calculates the coefficients A_l and B_l by using the two recursive equations (3.50) and (3.51). If a value is given to the amplitude of the transmitted field, A_N, all the other A_l and B_l can be calculated. The program gives the value of unity to A_N resulting in B_N having the value given in equation (3.49). Now that A_1 and B_1, of the metal region, are known, they are used to find the the reflectivity as given by equations (3.52)-(3.55). Next, the program calculates the amplitude of the incident magnetic field at the metal-prism interface that results in a unity amplitude magnetic field at the nonlinear-air interface as was assumed. The program then adjusts the coefficients A_l and B_l by multiplying them by the ratio of the amplitude given to the incident magnetic field and the one calculated from equation (3.53). Finally, the program computes the electric field components E_{xl} and E_{zl} at each layer of the active region and from that it computes $|E_l|^2$. The equations used in calculating E_{xl} and E_{zl} are given in (3.28) and (3.48) respectively. Then

$$|E_l|^2 = |E_{xl}|^2 + |E_{zl}|^2 \tag{3.56}$$

At this stage, the program modifies the dielectric constant of the nonlinear region by:

$$\varepsilon_l = \varepsilon_{bd} + \frac{\alpha |E_l|^2}{1 + \alpha \beta |E_l|^2} \tag{3.57}$$

and repeats the process until the difference between two successive iterations of the reflectivity is of order 10^{-8}. once convergence is obtained the program calculates the magnetic field profile throughout.

3.4.3 Comparison With Other Methods

In this section we will show that the program used in this thesis is correct and its results agree with the results obtained from closed-form formulas of the reflection coefficients. The verification will be divided into two parts, namely verification with linear structure and verification with structure having nonlinear layer.

3.4.3.1 Verification With Linear Structures

In order to compare the results of the program with analytical results , we will first derive an expression for the reflection coefficient of a three layer structure as the shown in figure (3.3). This is done for TM-polarized waves.

The three layer structure consists of a semi-infinite dielectric with dielectric constant ε_p in the superstrate, a metal with dielectric constant ε_1 and another semi-infinite dielectric in the substrate with dielectric ε_b. The thickness of the metal is assumed to be equal to d. The solution of the wave equation for the structure is given below in terms of the H_y field component. where given in equation (3.47). If we reduce that equation to three

$$H_y = \begin{cases} A_p e^{iq_p x} + R A_p e^{-iq_p x} & x<0 \\ A_1 \cos q_1(x-d) + B_1 \sin q_1(x-d) & 0<x<d \\ A_b e^{iq_b(x-d)} & x>d \end{cases} \tag{3.58}$$

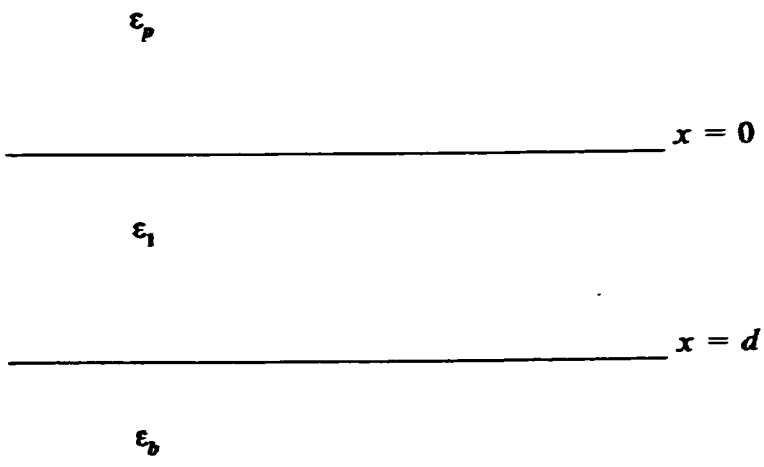

Figure (3.3) Three Layer structure used to compare the results of the our program and the analytic solution. ε_p and ε_b are dielectrics while ε_1 is metal.

Continuity of the H_y filed component at the interfaces x=0 and x=d results in:

$$(1 + R) A_p = A_1 \cos q_1 d - B_1 \sin q_1 d \qquad (3.59)$$

$$A_b = A_1 \qquad (3.60)$$

Similarly, the continuity of the E_z filed component, as given in equation (3.29) results in,

$$(1 - R) A_p = \left[\frac{q_1 \varepsilon_p}{i q_p \varepsilon_1} \right] \{ A_1 \sin q_1 d + B_1 \cos q_1 d \} \qquad (3.61)$$

and

$$B_1 = \frac{i q_p \varepsilon_1}{q_1 \varepsilon_b} A_b \qquad (3.62)$$

There are four unknowns, namely A_1 , A_p , A_b and B_1 and four equations: (3.59),(3.60),(3.61) and (3.62). Which can be solved for the amplitude reflection coefficient R. However, let us first assume that γ^{TM} is defined by equation (3.54) and ρ is defined by the following equation:

$$\rho = \frac{i\, q_p\, \varepsilon_1}{q_1\, \varepsilon_b} \tag{3.63}$$

Then γ^{TM} is given by:

$$\gamma^{TM} = \left[\frac{q_1\, \varepsilon_p}{i\, q_p\, \varepsilon_1}\right] \frac{\sin q_1 d + \rho \cos q_1 d}{\cos q_1 d - \rho \sin q_1 d} \tag{3.64}$$

The amplitude reflection coefficient is given by:

$$R = \frac{1 - \gamma^{TM}}{1 + \gamma^{TM}} \tag{3.65}$$

Example

Assume we have the three layer structure shown in figure (3.3) and the values of the dielectric constants are as follows:

$\varepsilon_p = 1.85$

$\varepsilon_b = 1.5$

$\varepsilon_1 = -16.0 + 0.5$

In addition, let the wavelength of the incident plane wave be .6323 μm and the angle of incidence be 61°. If we substitute these values into

equation (3.64), then equation (3.65) gives an amplitude reflection coefficient equal to:

$$R = 0.12851669222828299442E\text{-}01 - i\ 0.12718727019030734 4E\text{-}01$$

Now if we supply the self consistent program with all the values given in the example, it produces the following amplitude reflection coefficient:

$$R = 0.12851669222859398 1E\text{-}01 - i\ 0.12718727019031051 9E\text{-}01$$

Comparing the two values of the reflection coefficient, it can be seen that the two values are in good agreement with a difference of order 10^{-12}.

3.4.3.2 Verification With Structure Having Nonlinear Layer

Before trying to show the validity of the program with a nonlinear layer in the structure of investigation, it would be helpful to examine a sample output of the program as the iterative procedure is executed. The following is a sample output of the program for the values of dielectric constants given in the previous example and a saturable nonlinear medium described by equation (3.57) in the substrate. Where ε_{bd} is 1.5 and α,β are equal to 1 and 20 respectively. The angle of the incident wave is chosen to be very close to the resonance angle in order to make sure that the effect of the field on the refractive index is maximum. Considering the iterations it can be noticed that the first value is equivalent to the linear case calculated in the previous page.

Iterations	Reflection coefficient
0	0.12851669222828134OE-01 - i 0.12718727019030220 1E-01
1	0.19223461222112248 6E-01 - i 0.12737444387418867 5E-01
2	0.19229253638578807 9E-01 - i 0.12737424346528363 1E-01
3	0.19229258670889154 9E-01 - i 0.12737424329091382 4E-01
4	0.19229258675262437 1E-01 - i 0.12737424329072584 9E-01
5	0.19229258675262437 1E-01 - i 0.12737424329072584 9E-01

The accuracy of the program has also been verified in case: (a) when the field is very small and (b) when the field is very strong. These two cases are chosen for the following reasons. When the field is very small its effect on the refractive index of the nonlinear medium can be neglected. The structure can therefore be approximated by a linear one. Similarly, when the incident field is very strong the nonlinear medium will be saturated and can be considered again a linear one. This means we can apply the same formula of the previous section in order to check the accuracy of the amplitude reflection coefficient It must, however, be noted that there is one restriction on the program. The self-consistent program requires both the superstrate and substrate to be linear layers. To overcome this restriction we have assumed the existence of a linear fourth layer under the nonlinear region. This layer is assigned a dielectric constant equal to the background dielectric constant of the nonlinear medium. If we further assume that the thickness of the nonlinear layer is large enough, the incident field is not influenced by the existence of the fourth layer. If the incident field is very small the following amplitude reflection coefficient is obtained.

$$0.12851819832278011\mathit{7E}\text{-}01 - i\,0.12718728424100010\mathit{6E}\text{-}01$$

Which is approximately equal to the one calculated on page 67. On the other hand if we consider the other extreme i.e. the saturated case, with

the field incident at resonance angle of 62.4° we obtain from the program an amplitude reflection coefficient equal to:

$$-0.763497323867313449E\text{-}01 - i\,0.196328528480737300E\text{-}02$$

and from the three layer analytical equations (3.64) and (3.65) an amplitude reflection coefficient:

$$-0.763497338613156745E\text{-}01 - i\,0.196328507426075163E\text{-}02$$

It is clear that the two results above are approximately equal.

It is now necessary to verify the validity of the program at some intermediate field intensity between the very low and the very high values. However, there is no analytical formula for the amplitude reflection coefficient in this case and one must resort to the literature. The program used in reference [25] has been used for this purpose. The program used in this reference calculates the effective refractive index of a given structure containing a saturable nonlinear layer. In order to compare with the results of this program the resonance angles computed by our program were used to calculate the effective refractive index by,

$$n_e = n_p \sin 0$$

Table (3.1) shows some effective refractive index found from the two software at different incident field intensities.

Magnetic Intensity	The Implemented Program	Program of Ref{25}	Resonance Angle
1.0E-12	1.61726	1.61723	60.95
1.0E-08	1.62350	1.62306	61.35
1.0E-07	1.63269	1.63257	61.95
1.0E-06	1.63723	1.63708	62.25

Table (3.1) Table showing the comparison between the effective refractive indices of the implemented program and the program which was used by reference [25].

CHAPTER 4

REFLECTIVITY MODULATION

4.1 INTRODUCTION

Now that we have developed the necessary background materials in the two preceding chapters, we present the results obtained for the structure of figure (1.1) which is reproduced again as figure (4.1) in this chapter. In this chapter all the parameters, such as the metal thickness and type and the nonlinear medium type and thickness, of figure (4.1) are selected. The surface plasmon resonance curves are also described. Furthermore, the relationship between reflectivity and the intensity of the two incident beams in this configuration is investigated.

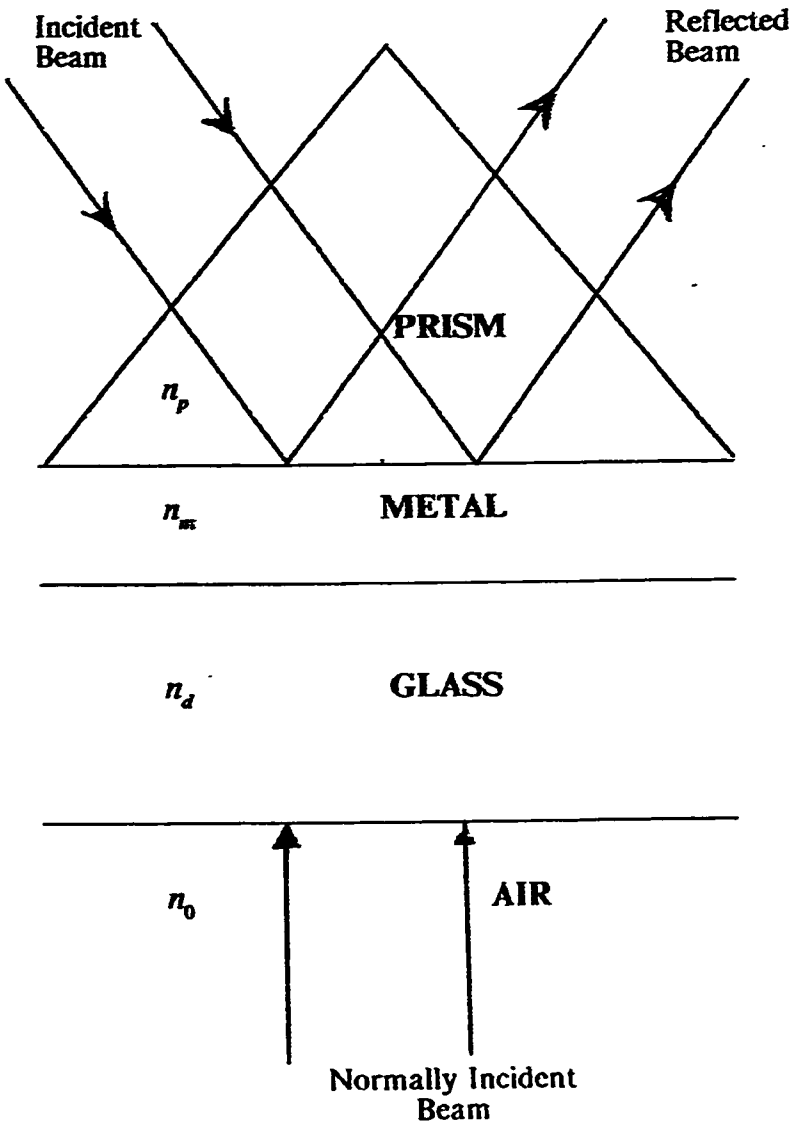

Figure (4.1) The structure used for reflectivity modulation using a normally incident beam.

It is appropriate at this stage to restate restate the problem under investigation. The aim of this thesis is to show reflectivity modulation of a beam by using another normally incident beam. In other words, we are attempting transfer information from the normally incident beam of given wavelength into another one with the same or different wavelength incident obliquely through the prism into the structure.

4.2 PARAMETERS OF THE MODULATOR

4.2.1 Introduction

The linear part of the refractive index of the nonlinear region is taken to be 1.5 corresponding for example to CS_2 while the refractive index of the the prism material is taken to be 1.85. In plasmon polariton resonance it is practiced to choose a prism of high refractive index. The value of 1.85 is obtained in a TaFD9 prism. The dielectric constant of the metal used in the structure, silver, is (-16 + i 0.5) at $\lambda = 0.633\mu m$.

4.2.2 Selection of the Metal Thickness

It has been mentioned in chapter 2 that the dip of the surface plasmon resonance curve depends on the thickness of the metal. Proper

choice of the metal layer thickness is important in achieving a very small values of the reflectivity at the resonance angle. Figure (4.2) shows surface plasmon resonance curves for five different values of the metal thickness. These values show the reflectivity at the resonance thickness, at a thickness greater than that of resonance and a at thickness smaller than that of resonance. It is clear from the figure that for values smaller than the resonance metal thickness the curves become flatter while for the cases of greater thicknesses the curves are sharper. In both cases the dip of the curve is smaller than that of the resonance thickness. The resonance thickness of the metal has been chosen to be 55 nm giving the value of reflectivity at resonance of order 10^{-3} .

4.2.3 Selection of the Nonlinear Layer Thickness

Two criteria are used in the selection of the active region thickness. The first is that the electric field intensity due to the beam incident from below should be as large as possible and the second is that the surface plasmon polariton should decay completely within the nonlinear layer. The first criterion is used because the electric field intensity in the nonlinear layer changes the refractive index of that layer and it is desirable to obtain a change in the refractive index of this layer with the

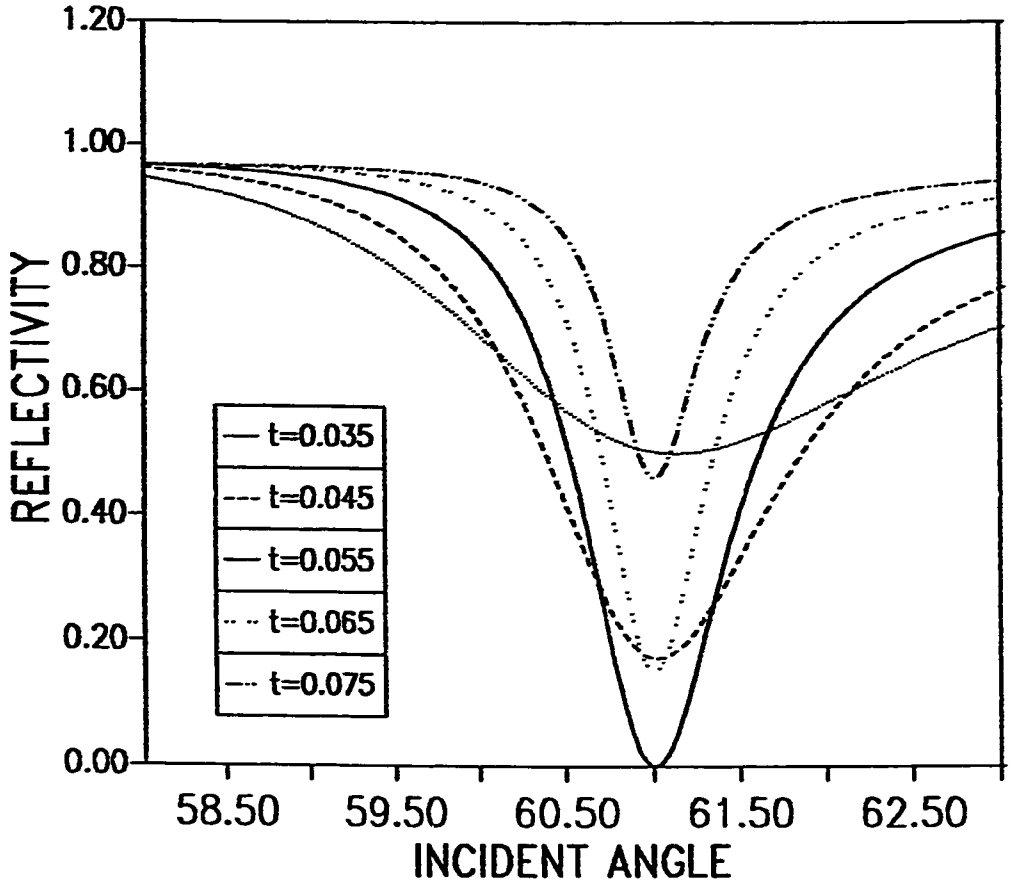

Figure (4.2) Tuning the thickness of the metallic layer.

smallest possible incident light power. The second restriction is imposed for the purpose of removing the effect of the substrate. In order to meet the above two requirements the nonlinear term in the dielectric function of the active region is suppressed. The thickness of the nonlinear region is changed gradually and the electric field intensity calculated is shown figure (4.3). The figure shows that the electric field intensity in the nonlinear layer undergoes resonance at a certain thickness. At this thickness the electric field intensity is enhanced. Changing the thickness away from that of resonance the electric field intensity drops. The reason for this resonant behavior is that the incident field is reflected by the metal and the combination of the incident field and the reflected field forms standing wave pattern inside the active layer. As the thickness increases resonance is observed periodically for changes of the thickness equal to $\frac{\lambda_d}{2}$. Where λ_d is the wavelength inside the dielectric layer. In our case, the first three resonances occurred at thicknesses of 0.08 μm , .29 μm and .50 μm . A simple formula that governs the resonance thickness is,

$$d_{res} = d_0 + \frac{\lambda_d}{2} \qquad (4.1)$$

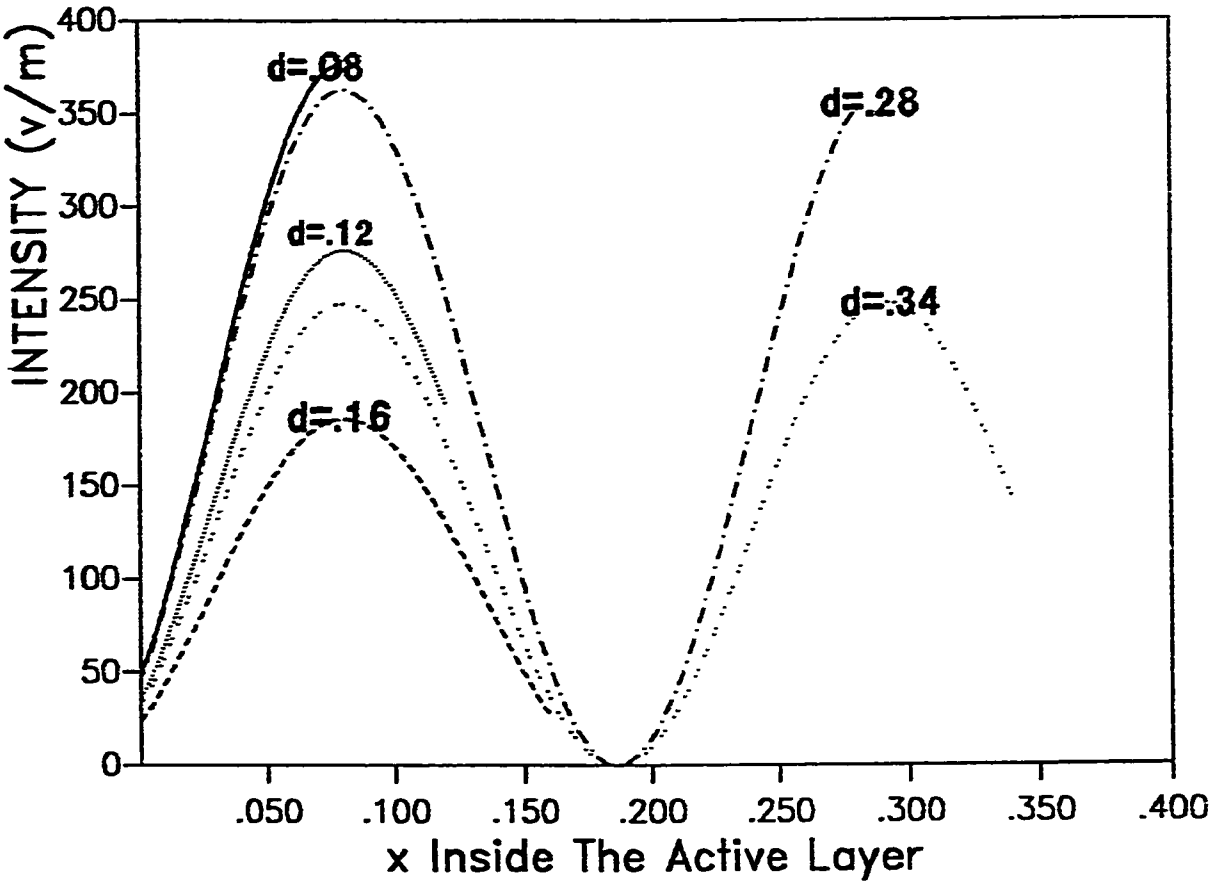

Figure (4.3) Standing wave patterns inside the active layer for different thickness of this layer.

Where d_0 is equal to the thickness of the first resonance (0.08) and λ_d is the wavelength inside the nonlinear layer. In the present case $\lambda_d = 0.4219\ \mu m$.

The second requirement, namely that the plasmon polariton field should decay completely within the active region was found to be satisfied with the resonance thickness of 0.5 μm. At this thickness the ratio of the field at the air-dielectric interface to that at the metal-dielectric interface is less than 10^{-4}. The value $d = 0.5\ \mu m$ thus guarantees that the field decays inside the nonlinear medium.

4.2.4 Nonlinearity of The Active Layer

If the dielectric constant of a given medium changes with the electric field, the medium is refereed to as a nonlinear medium. In the present thesis the field dependence of the dielectric constant arises from the third order nonlinear term in the polarization vector. For nonlinear media the constitutive relationship is given by [26],

$$\overline{D} = \varepsilon_0 \overline{E} + \overline{P} \qquad (4.2)$$

where $\overline{P}$ it self is represented by [26]

$$P = \chi_j E_j + 2\chi_{jk} E_j E_k + 4\chi_{jkl} E_j E_k E_l + \cdots \qquad (4.3)$$

In this thesis the nonlinearity of the material is assumed to be due to the third order term, χ_{jkl}, of equation (4.3). Assuming that χ_{jk} and all the terms higher than the third order to be zero results in the following equation,

$$\overline{D} = (\varepsilon_0 + \chi_j + 4\chi_{jkl}|E|^2)\overline{E} \qquad (4.4)$$

Writing equation (4.4) in the form

$$\varepsilon_d = \varepsilon_{db} + f(|E|^2)$$

where ε_{db} is the background dielectric constant, it is seen that

$$f(|E|^2) = \alpha |E|^2 \qquad (4.5)$$

where α is a constant. This form is in fact the Kerr nonlinearity. However , the Kerr nonlinearity does not account for the saturation exhibited by realistic materials. For this reason two phenomenological forms of saturable dielectric functions are commonly employed. They are represented by [27]

$$f(|E|^2) = \frac{\alpha |E|^2}{1 + \alpha \beta |E|^2} \qquad (4.6)$$

and

$$f(|E|^2) = \alpha\,(1 - exp(-\gamma\,|E|^2) \qquad (4.7)$$

It is seen that both expression (4.6) and (4.7) lead to saturable values given by $\frac{1}{\beta}$ and α respectively. In this thesis equation (4.6) is used to represent the saturable nonlinear medium in the structure of figure (4.1). Throughout the thesis the electric field is scaled so that the value of α is equal to unity. On the other hand β is given a value equal to 20. This results in a maximum change in the dielectric constant equal to 0.05. This is equivalent to 2.2 percent maximum increase in the refractive index of the active layer. Later in this chapter the effect of β on the reflectivity will be investigated.

4.3 REFLECTIVITY INVESTIGATION

4.3.1 The Relation Between Reflectivity and Angle of Incidence

Having decided all the parameters of the structure under investigation, figure (4.1), we are ready to analyse this structure and the possibility of light by light modulation. The aim of the first analysis done on the structure was to find the angle at which a surface plasmon

Figure (4.4) Angular scanning of the upper incident on the structure at low power.

polariton is excited. But we know that the angle depends on the field existing in the active layer. As a result, we assumed that the nonlinear layer acts as a linear layer, in other words the intensity is very low. After that we looked at the effect of increasing the field on this resonance angle. Assume now that the structure in figure (4.1) contains only one incident beam, namely the upper beam and that the intensity of this beam is very low. Running the self consistent scheme under these conditions and scanning the angle incidence from an angle lower than the critical angle and greater than the expected resonance angle, we found the result shown in figure (4.4). The critical angle was calculated to be equal to $\sin(1/1.85) = 32.72°$ and the angle at which the plasmon is excited was calculated by using equation (2.2). But we know that equation (2.2) gives only the propagation constant of the plasmon polariton β. In order to calculate the resonance angle we have to use the following equation.

$$\beta = k_0 n_p \sin\theta_0 \qquad (4.8)$$

But β on the other hand can be found from $\beta \approx k n_e'$, where n_e' is the real part of the effective refractive index of the structure when the plasmon polariton is excited. From equation (2.2) n_e' was found to be equal to 1.6179 resulting in an angle of resonance equal to 60.99 degrees. Looking in figure (4.4) we can see the critical angle is approximately

equal 32.7 degrees and the angle of resonance at low power is 60.95 degrees. In addition to that we see in figure (4.4) a third resonance at an angle approximately equal 45 degrees. This angle represents the angle at which the guided wave TM_0 is excited. To make sure of that we plotted the magnetic field at that angle and it showed the well known curve of a TM_0 . The curve is shown in figure (4.5). In addition, we used the program which was used in reference [25] and it gave approximately the same n_e . Having a second look at figure (4.4), we notice that the dip due to the excitation of surface plasmon is smaller than that of the TM_0 . This is due to the choice of the thickness of the metallic layer. In other words, by another choice of metal thickness, we can decrease the dip of the TM_0 while increasing that of the plasmon polariton: make the structure prefer the excitation of the TM_0 more than the excitation of the plasmon. Figure (4.6) shows a close look of the surface plasmon resonance curve. The value of the reflectivity at resonance angle was of the order 10^{-4} . Although this value can be lowered by tuning the thickness of the metallic layer more, for our application this value is more than sufficient because we are analysing a device that will amplitude modulate a beam of light and the device that will sense the reflected beam will interpret both values as being a zero.

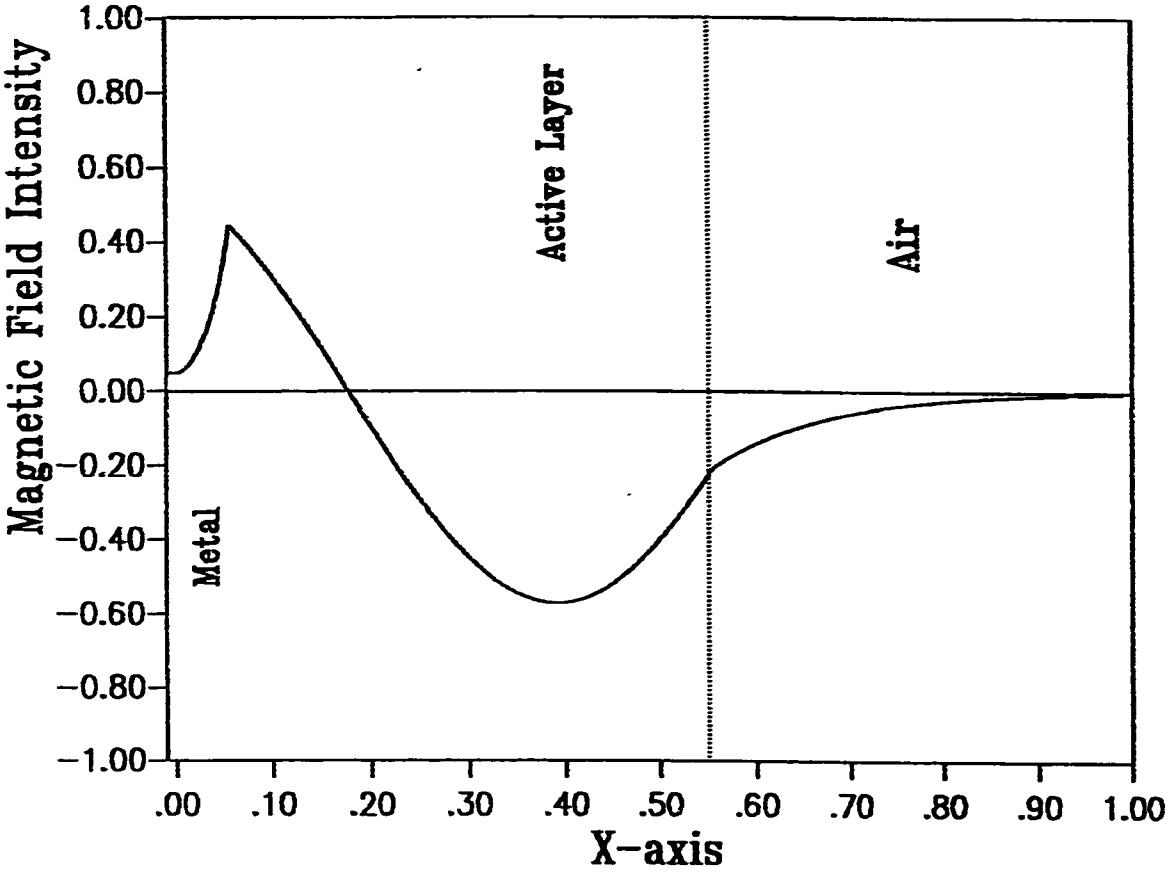

Figure (4.5) A plot of the magnetic field intensity H_y incident through the prism for the guided wave TM_0.

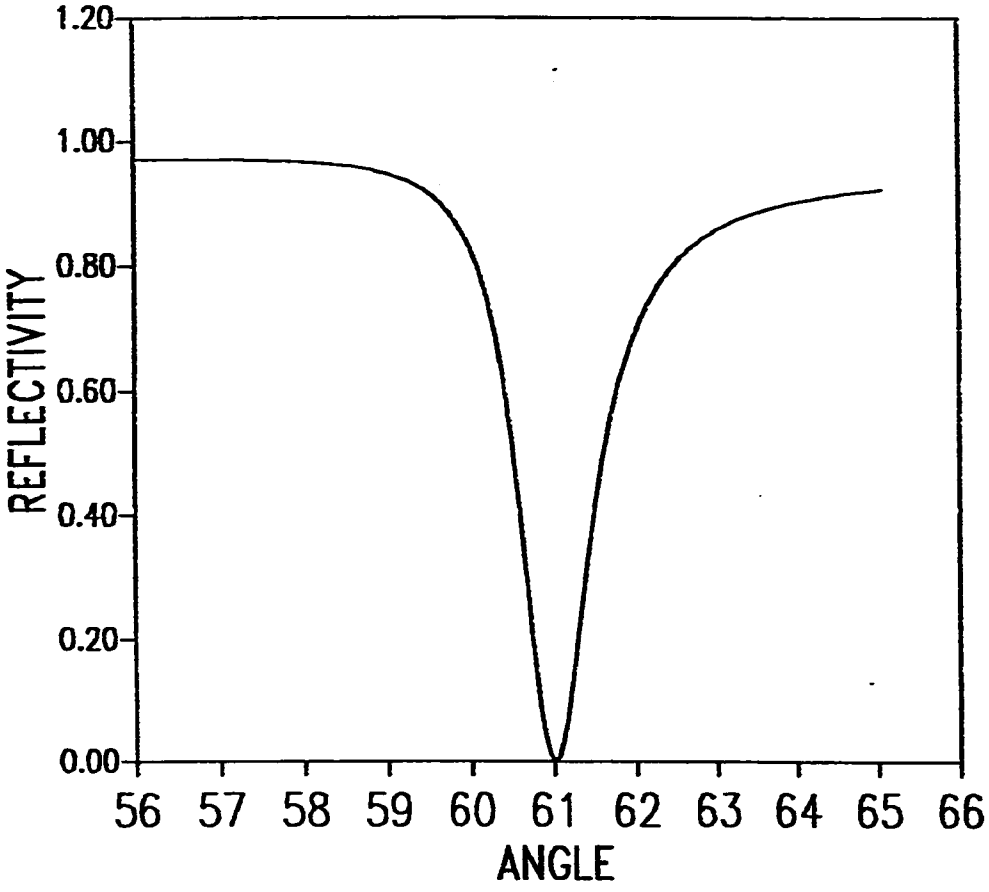

Figure (4.6) Reflectivity vs incident angle at low power.

4.3.2 The Relation Between Reflectivity and Intensity of a Beam

Assume now that the intensity of the incident upper beam is increased gradually. The beam will start, in this case changing the refractive index of the active medium and this will result, as stated in the first chapter in changing the resonance angle. The result of analysis is shown in figure (2.7). It can be noticed from this figure that the surface plasmon resonance curve shifts its position as the intensity of the incident beam increases. Another point that is noticed from figure (4.7) is that after some intensity of the order 0.1 or greater, the plasmon sees a saturated medium and the resonance angle is not changed with the changes in the intensities of the incident beam. The resonance angle after the saturation of the nonlinear layer is approximately equal to 62 degrees. Which means that for any intensity the resonance angle is between 60.95 and 62 degrees. For our case this beam was chosen to have very low intensity so that it will not affect the modulation which will be due to the lower beam. If the angle of incidence of the upper beam is fixed at an angle equal to the low power resonance angle and its intensity is increased, the amplitude of the reflected beam will under-go changes that range between zero and 0.9. In other words, it can switch itself if its intensity is increased. This is shown in figure (4.8). Assume now that we fixed the angle of incidence beam at a value greater than

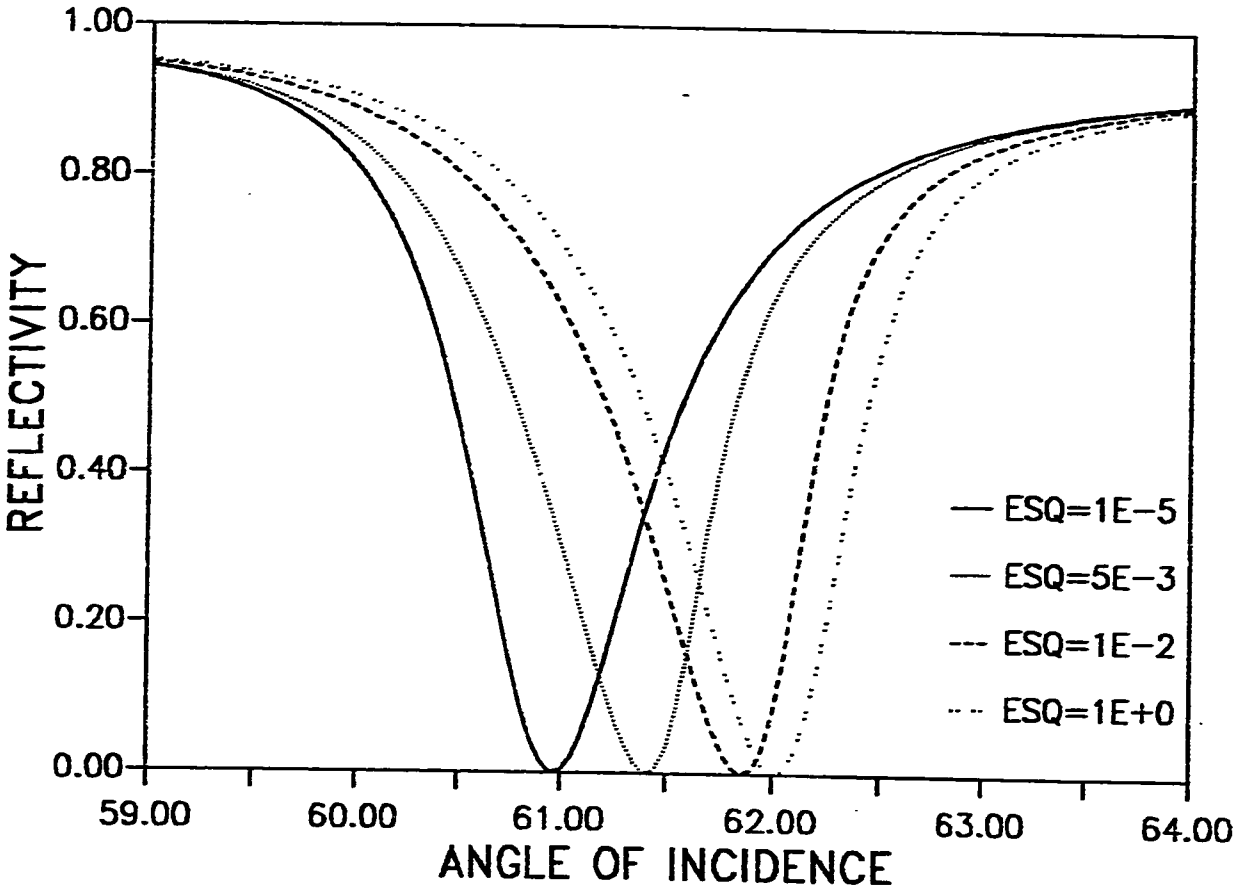

Figure (4.7) Reflectivity vs incident angle for different values of intensity of the upper beam.

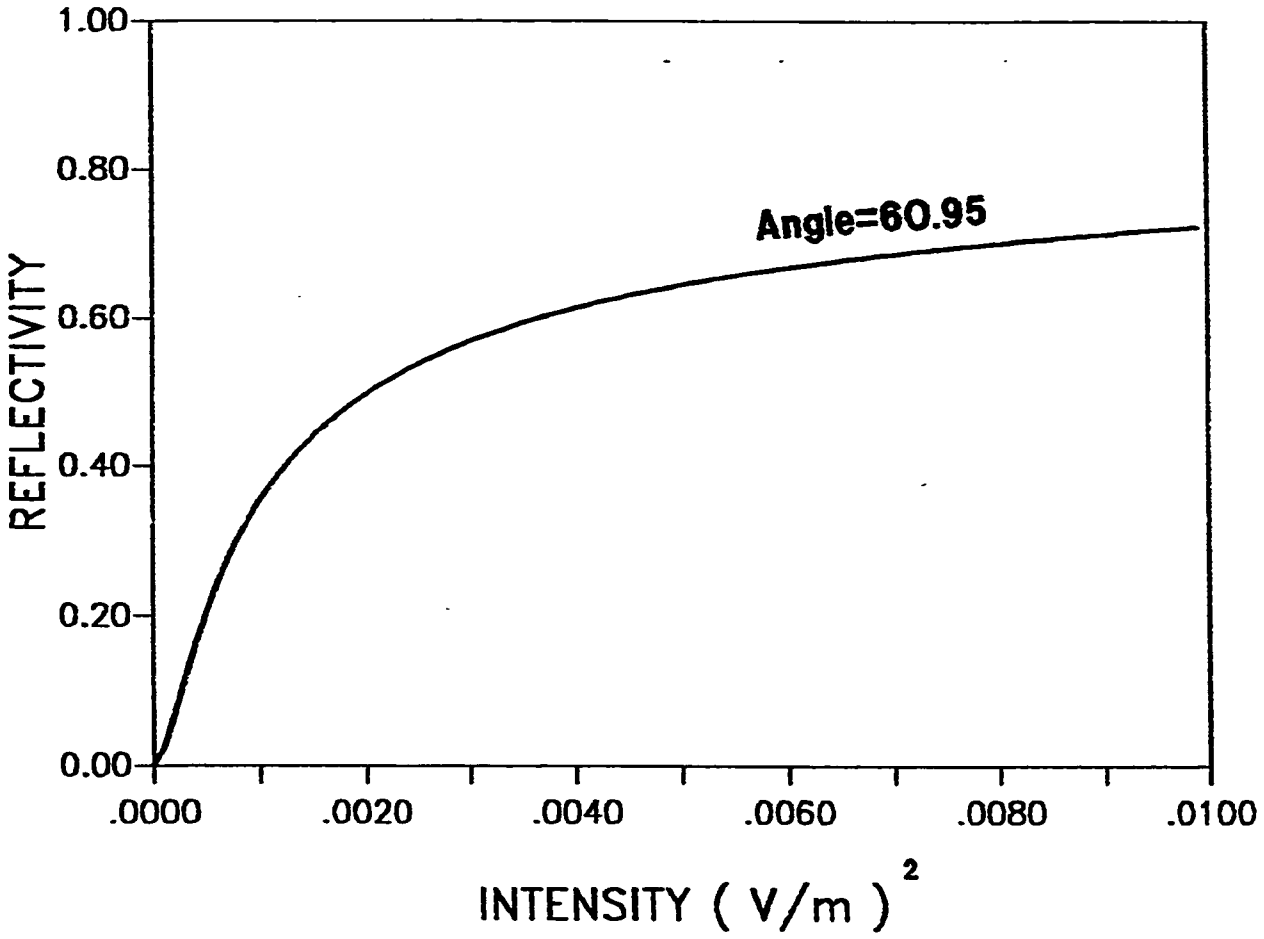

Figure (4.8) The effect of increasing the upper beam intensity on its reflectivity for fixed angle equal to the low power resonance angle.

that of the low power and smaller than that of the saturated case, say 61.50 degrees. In this case increasing the intensity of the incident beam will result in changing the reflectivity in such a way that it passes through a resonant angle, shown in figure (4.9). It shows also that at very low power the reflectivity was about 0.45 and for large intensities the reflectivity did not reach to 0.9 as in the first case instead it takes a constant value of about 0.4. If we had chosen the angle of incident close to the low power resonance angle the curve could have reached a value of a reflectivity equal to 0.9. While if we chose a values close to the resonance angle after saturation, the reflected beam will pass through a resonance by increasing the intensity of the incident beam but it will saturate at very small value of the reflectivity. Figure (4.10) shows the reflectivity vs intensity for the third case, incidence angle smaller than low power resonance angle. In this case the curve does not pass through resonance and the reflectivity value at low power depends on how close is our choice of the angle of incidence. It ranges from very small values, when close to low power resonance angle, to about 0.9, when very far from that angle.

Assume that another beam is incident into the structure from below and the changes in the dielectric constant of the active layer are due to the this beam (modulating beam). The upper beam (to be modulated)

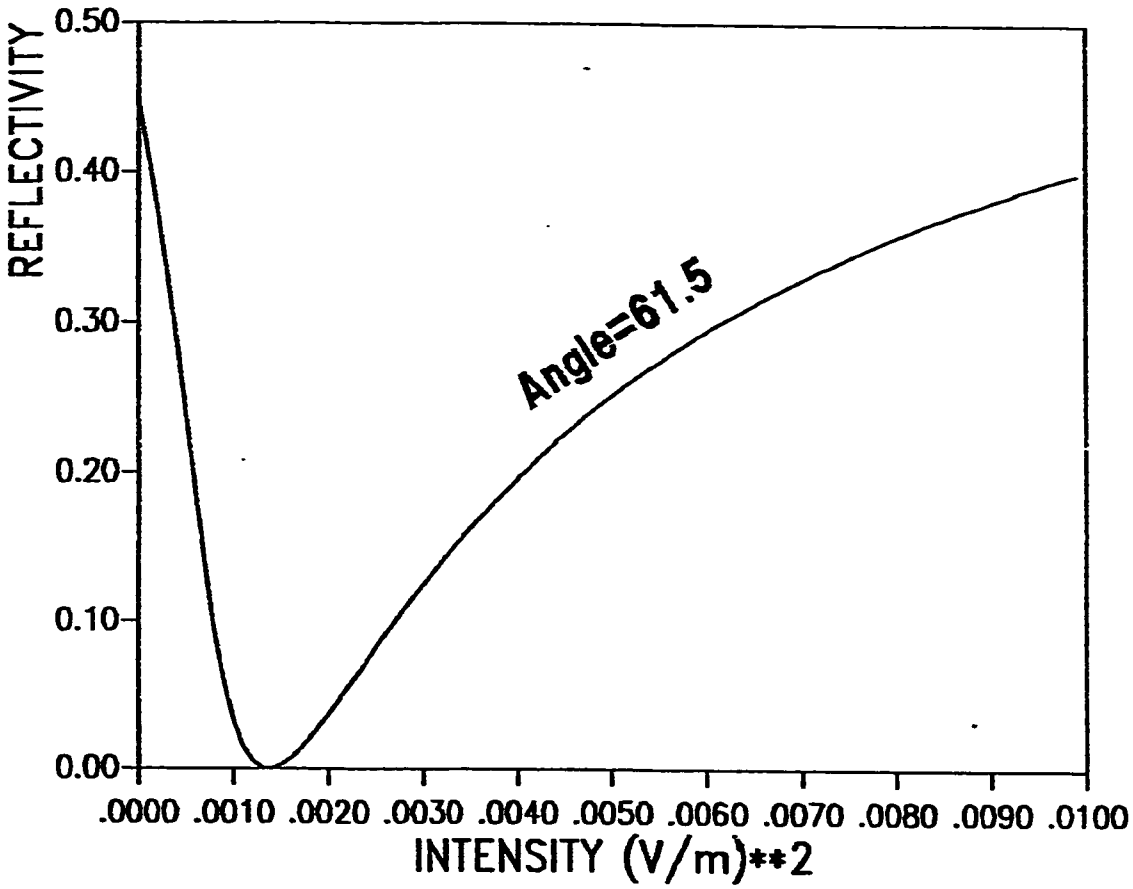

Figure (4.9) The effect of increasing the upper beam intensity on its reflectivity for fixed angle greater than the low power resonance angle.

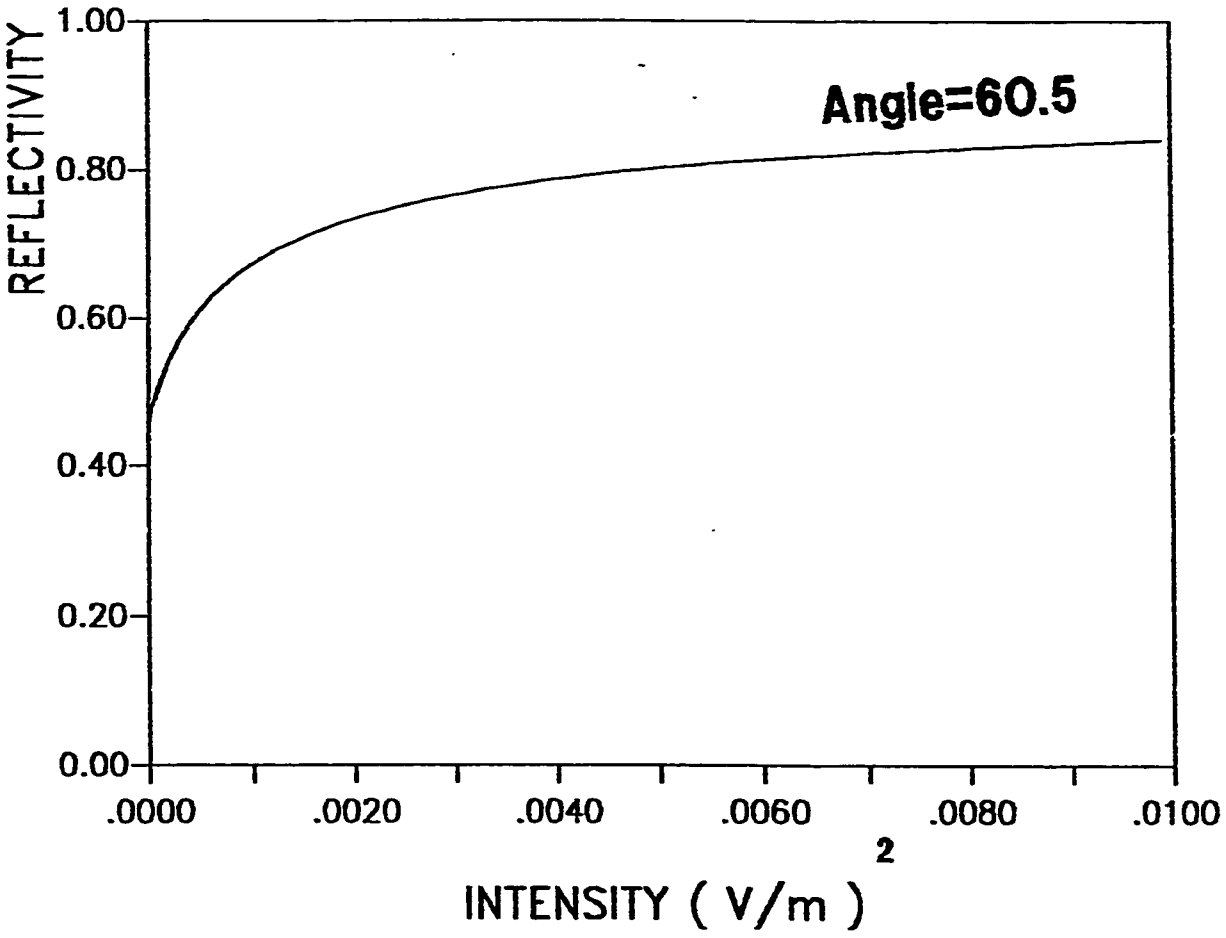

Figure (4.10) The effect of increasing the upper beam intensity on its reflectivity for fixed angle smaller than the low power resonance angle.

is assumed to have a fixed intensity. A similar analysis to the above can be carried out. But this means that the effects of the two beams must be accounted for at the same time. But because of our assumption that the intensity of upper beam is very low and does not affect the nonlinear medium, we can divide the task into two parts. In the first part, the lower beam is incident on the structure and it sees the active layer as a saturable nonlinear medium and it changes its refractive index according to its value. This analysis is done by the use of the self-consistent scheme. While in the second part the upper beam sees a linear structure in which the active layer has a grade index instead of a step index. This graded index comes from the first part. The result of these analyses is presented in figure (4.11). This figure shows the reflectivity of the upper beam as the intensity of the second beam is changed. The values of the fixed angle for each curve was chosen in a way to have values smaller, larger and equal to the low power resonance angle.

Finally, the effect of saturation level on the reflectivity is investigated. To show this effect it was chosen that the obliquely incident beam be incident at an angle equal to the low power resonance angle. The intensity of the lower beam is then increased gradually. This is done for different levels of saturation. Figure (4.12) shows the reflectivity as

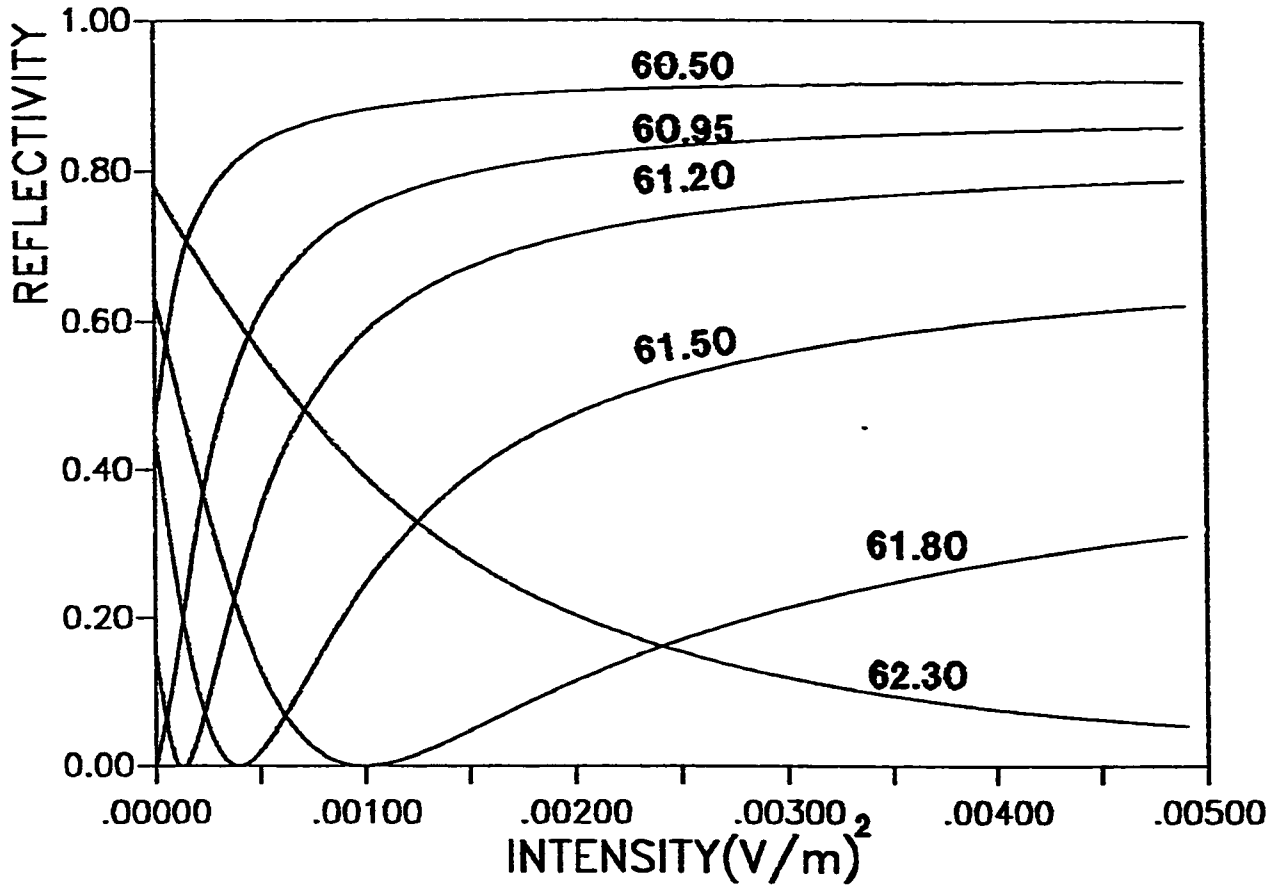

Figure (4.11) The effect of increasing the upper beam intensity on its reflectivity for different angles of incidence.

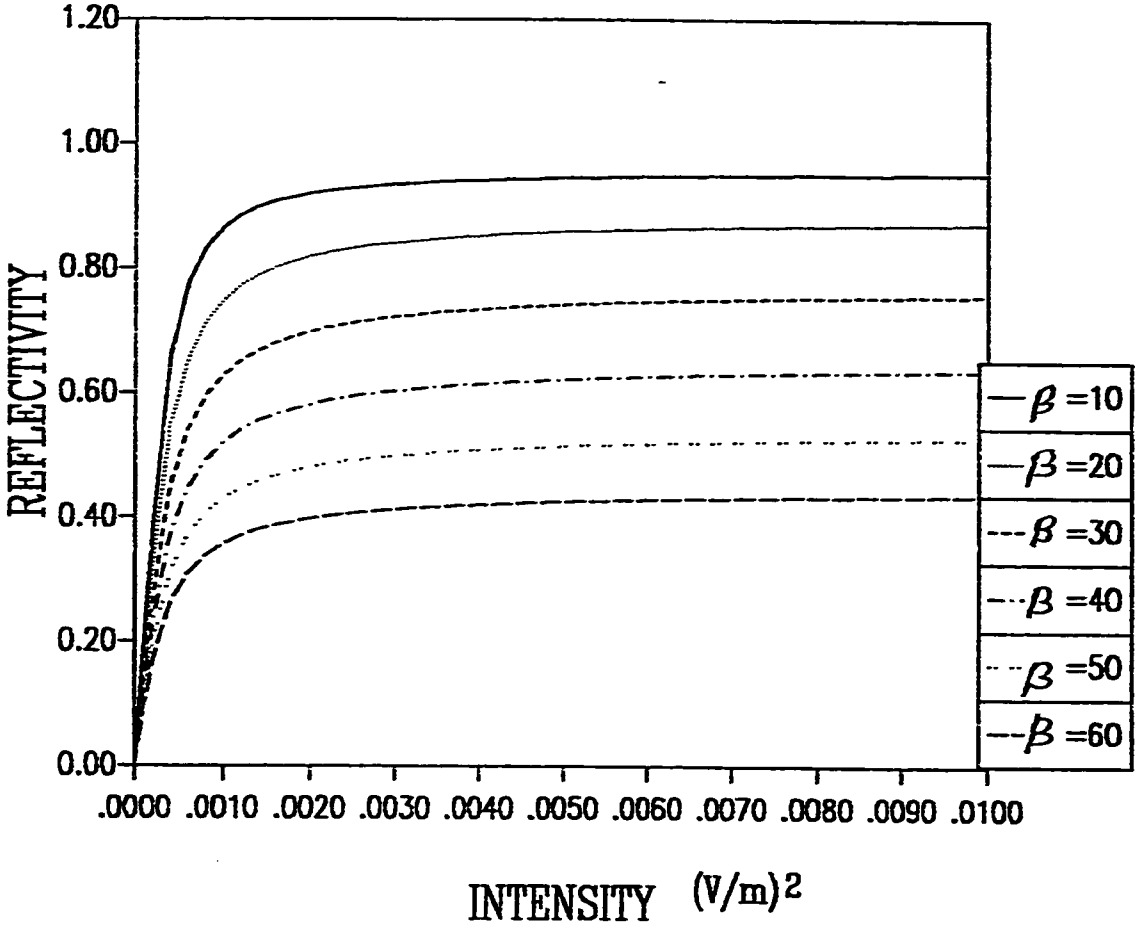

Figure (4.12) The effect of saturation level on the reflectivity of the upper beam incident at the low power resonance angle.

the intensity of the lower beam increases for different levels of saturation. It is seen from the figure that the modulator prefers high level of saturation to achieve nearly one difference between the on and off of the upper beam.

CHAPTER 5

CONCLUSION AND FUTURE WORK

5.1 CONCLUSION

In this thesis an all optical reflectivity has been demonstrated. The structure of the modulator consists of a thin metallic layer deposited on the base of a prism. The metallic layer is also coated by a nonlinear medium. The operation of this modulator can be summarize by the following steps. (1) A beam of a very low intensity is incident through the prism on to a metal layer and reflected. This will excite a surface plasmon polariton at the lower layer of the metallic layer if the matching conditions are satisfied. (2) The modulating beam is incident to the structure from the bottom. (3) If the intensity of the modulating signal is very small the upper beam will not be observed from the prism side i.e

no reflection. (4) But If the intensity of the modulating signal is large the upper beam will be reflected and will be observed from the prism side.

From the analysis done on the modulator the following conclusion were reached. Only the strong beam (the modulating beam) caused the modulation of the upper beam. Depth of modulation up to 100 % is shown to be obtainable. It was found also that increasing the saturation level will increase the depth of modulation. Although the same frequency was used for both beams, it may not be necessary. Finally in this thesis the self-consistent scheme was demonstrated for TM polarized waves.

5.2 FUTURE WORK

Some of the possible future works are summarized in the following.

(1) Future work should optimize the parameters of the structure in particular the thickness of the active region and its type.

(2) It should also study the dynamics of the modulator (speed of modulation.

(3) One can also investigate using the structure to study the nonlinearity of a material.

APPENDIX

THE SELF-CONSISTENT PROGRAM USED IN THE THESIS

ACCOUNTING FOR THE LOWER BEAM
NONLINEAR CASE

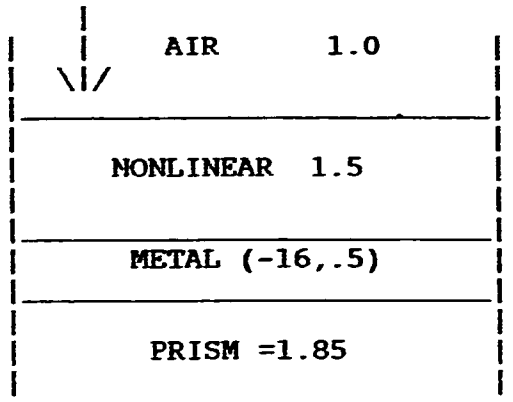

ACCOUNTING FOR THE UPPER BEAM
NLINEAR CASE

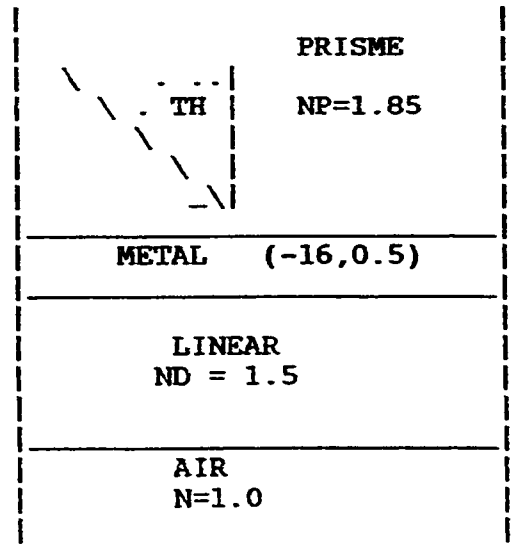

SEFLF-CONSISTENT PROGRAM

THIS PROGRAM COMPUTES THE REFLECTION COEFFECINT OF A PLANE
WAVE FROM A MULTILAYER STACK WHICH CONTAINS NONLINEAR MEDIA.

—— ONLY "TM" WAVES ARE ACCOUNTED FOR————

THE PROGRAM CAN EASILY BE MODIFIED TO ACCOUNT FOR TE WAVES.

FOR TM WAVES RHO = RATIO OF RELATIVE PERMITTIVITIES.
THE MEDIUM OF INCIDENCE IS CALLED SUPERSTRATE.
THE MEDIUM OF TRANSMISSION IS CALLED SUBSTRATE.
THE MEDIUM IMMEDIATELY BELOW THE SUPERSTRATE IS
MEDIUM ONE,THEN TWO,ET
THE MEDIUM ABOVE THE SUBSTRATE IS MEDIUM NN.
TH = ANGLE OF INCIDENCE WITH RESPECT TO THE NORMAL.
NN = TOTAL NUMBER OF LAYERS.
P(1) = POSITION OF THE FAR END OF LAYER 1.
P(2) = POSITION OF THE FAR END OF LAYER 2 , AND SO ON.
P(NN) = POSITION OF THE FAR END OF THE LAST LAYER.
NN = TOTAL NUMBER OF LAYERS NOT COUTING THE SUPER OR THE
SUBSTRATE.
NSUP = SUPERSTRATE INDEX.
NSUB = SUBSTRATE INDEX.

LAMBDA = FREE SPACE WAVELENGTH.

K = FREE SPACE WAVE NUMBER.

P(I) = ARRAY THAT CONTAINS THE POSITIONS OF THE FAR

ENDS OF THE LAYER.

THE SUPERSTRATE OCCUPIES THE REGION X < 0.

N(I) IS AN ARRAY CONTAINING THE REFRACTIVE INDICES

OF THE VARIOUS LAYER.

N(1) IS THE INDEX OF THE LAYER ADJACENT TO THE

SUPERSTRATE,AND N(NN) IS THE INDEX OF THE FINAL

LAYER WHICH IS ADJACENT TO THE SUBSTRATE.

FIRST THE COEFFECENTS OF THE SINE AND THE COSINE

FUNCTIONS ARE COMPUTED THEN THE FIELD DISTRIBUTION

IS DETERMINED,BY MEANS OF THE SUBROUTINE FIELD(F,X).

THE FIELD IS NORMALIZED IN SUCH A WAY THAT THE

INCIDENT FIELD AMPLITUDE IS EQUAL TO UNITY.

THE PROGRAM STARTS HERE

```
      IMPLICIT REAL*8(A-H,O-Z)
      COMPLEX*16 NSQ(1010),NSQ2(1010),NSUP,NSUPSQ,NSUB
      COMPLEX*16 NSUBSQ,A(1010),B(1010),Q(1010)
      COMPLEX*16 RHO,NZ,NZSQ,EX,EZ,ESQ(1010)
      COMPLEX*16 QP,QB,C,RATIO,REFLCO,H0,F,T
      REAL*8 P(0:1010),K,LAMBDA,E0DSQ,E0DSQ2,TH22(10)
      REAL*4 X
C
C   DEFINING FIFERENT ANGLE OF INCIDENCE OF
C           THE UPPER BEAM
C
      TH22(1) = 60.5
      TH22(2) = 60.95
      TH22(3) = 61.2
      TH22(4) = 61.5
      TH22(5) = 61.8
      TH22(6) = 62.0
      TH22(7) = 63.0
      TH22(8) = 64.0
      TH22(9) = 67.5
      TH22(10) = 68.0
```

```
C     WRITE(16,*) 500

      DO 888 JTH = 1,8

C
C  ENTER THE ANGLE OF THE NORMALLY INCIDENT BEAM.
C
         TH = 0.0

C
C  ENTER INTENSITY OF THE NORMALLY INCIDENT BEAM
C       AT THE METAL/PRISM INTERFACE
C
         E0DSQ = 1.D-9
C
C  THE THICKNESS OF THE METAL
C
         W1 = .055
C
C'NUMBER ENTER LAYERS NN NOT INCLUDING
C  THE SUBSTRATE AND THE SUPERSTRATE
C  LL IS THE LAYERS WITHIN THE NONLINEAR
C  LAYER AND MM IS # OF LAYER
C  WITHIN THE METALLIC LAYER
C
```

```
1111  LL=200
      MM=20
      NN=LL+MM
      RRP=2
C
      PI=2.D0*DASIN(1.D0)
      C=DCMPLX(0.D0,1.D0)
      LAMBDA=0.6328D0
      NSUP=DCMPLX(1.D0,0.D0)
      NSUPSQ=NSUP**2
      NSUB=DCMPLX(1.85D0,0.D0)
      NSUBSQ=NSUB**2
      K=2.D0*PI/LAMBDA
      NZ=NSUP*DSIN(TH*PI/180.D0)
      NZSQ=NZ*NZ
            H0DSQ=((1.D0/120.D0*PI)**2)*E0DSQ
            H0D=DSQRT(H0DSQ)
C
C  WIDTH OF THE NONLINEAR REGION
C
      WIDTH=0.500D0
      FMM=FLOAT(MM)
      FLL=FLOAT(LL)
```

```
      WT = WIDTH/(FLL)
      WTM = W1/(FMM)
C
      DO 501 I = 1,LL
          P(I) =  FLOAT(I)*WT
          NSQ(I) = 1.5D0**2
501   CONTINUE
C
C
C ENTER REFRACTIVE INDEX DISTRIBUTION
C
      DO 501 I = LL + 1,NN
          P(I) = WIDTH + FLOAT(I-LL)*WTM
          NSQ(I) = DCMPLX(-16.D0,.5D0)
501   CONTINUE

432   DO 577 I = 1,NN
          Q(I) = K*CDSQRT(NSQ(I)-NZSQ)
577   CONTINUE

      QP = K*CDSQRT(NSUPSQ-NZSQ)
      QB = K*CDSQRT(NSUBSQ-NZSQ)
C
          RHO = NSQ(NN)/NSUBSQ
```

```
      A(NN) = 1.D0
      B(NN) = RHO*C*QB/Q(NN)
      DO 12 I = NN,2,-1
            RHO = NSQ(I-1)/NSQ(I)
      A(I-1) = A(I)*CDCOS(Q(I)*(P(I)-P(I-1)))
     $-B(I)*CDSIN(Q(I)*(P(I)-P(I-1)))
      B(I-1) = A(I)*CDSIN(Q(I)*(P(I)-P(I-1)))
     $+B(I)*CDCOS(Q(I)*(P(I)-P(I-1)))
      B(I-1) = B(I-1)*RHO*Q(I)/Q(I-1)
12    CONTINUE
            RHO = NSUPSQ/NSQ(1)
      RATIO = A(1)*CDSIN(Q(1)*P(1)) + B(1)*CDCOS(Q(1)*P(1))
      RATIO = RATIO/(A(1)*CDCOS(Q(1)*P(1))-B(1)*CDSIN(Q(1)*P(1)))
      RATIO = RATIO*RHO*Q(1)/QP/C
      REFLCO = (1.D0-RATIO)/(1.D0+RATIO)
      H0 = (A(1)*CDCOS(Q(1)*P(1))-B(1)*CDSIN(Q(1)*P(1)))
      H0 = H0/(1.D0+REFLCO)
       RRN = CDABS(REFLCO)**2
C     WRITE(6,*)TH,REFLCO
C     WRITE(6,*)NSS,TH,CDABS(REFLCO)**2
C
C ADJUST THE FIELD AMPLITUDE
C H0 = COMPUTED INCIDENT MAGNETIC FIELD AMPLITUDE
```

```
C H0D=DESIRED OR ACTUAL INCIDENT MAGNETIC FIELD AMPLITUDE
C
      DO 72 I=1,NN
        A(I)=(H0D/H0)*A(I)
        B(I)=(H0D/H0)*B(I)
72    CONTINUE
C
C COMPUTE EX AND EZ THEN E**2 IN EACH LAYER OF
C       THE NONLINEAR MEDIUM
C
      P(0)=0.0
      DO 502 I=1,NN
      EX=A(I)*CDCOS((P(I)-P(I-1))*Q(I)/2.D0)-
     $B(I)*CDSIN((P(I)-P(I-1))*Q(I)/2.D0)
      EX=EX*120.D0*PI*NZ/NSQ(I)
      EZ=A(I)*CDSIN((P(I)-P(I-1))*Q(I)/2.D0)+
     $B(I)*CDCOS((P(I)-P(I-1))*Q(I)/2.D0)
      EZ=EZ*C*120.D0*PI*Q(I)/K/NSQ(I)
      ESQ(I)=CDABS(EX)**2+CDABS(EZ)**2
502   CONTINUE

C  COMPUTE THE NEW REFRACTIVE INDEX PROFILE
```

```
      ALPHA=1.D0
      BETA=20.D0
      DO 503 I=1,LL
      NSQ(I)=1.5D0**2+ALPHA*ESQ(I)/(1.D0+BETA*ALPHA*ESQ(I))
 503  CONTINUE

       IF(ABS(RRP-RRN).GE.1.0d-10) THEN
          RRP=RRN
          GO TO 432
       ENDIF

C_________%%%%%%%%%%%%%%%%%%%%%%%%%%%%%%%_____________ __
C#######################################################
C%%%%%%%%%%%%%%%%%%%%%%%%%%%%%%%%%%%%%%%%%%%%%%%%%%%%%%%
C
C          LINEARIZED  PART OF THE PROGRAM
C
C
C
C  INTENSITY OF THE UPPER BEAM
      E0DSQ2=1.D-8

C 'ENTER WIDTH OF FIRST LAYER (METAL)')
```

```
      W1 = .055
C
C 'NUMBER ENTER LAYERS NN')
      LL = 200
      MM = 20
      NN = LL + MM
C
C
C  ENTER TH OF THE UPPER BEAM
C
      TH = TH22(JTH)

      NSUP = DCMPLX(1.85D0,0.D0)
      NSUPSQ = NSUP**2
      NSUB = DCMPLX(1.0D0,0.D0)
      NSUBSQ = NSUB**2
      K = 2.D0*PI/LAMBDA
      NZ = NSUP*DSIN(TH*PI/180.D0)
      NZSQ = NZ*NZ
      H0DSQ = ((1.D0/(120.D0*PI))**2)*E0DSQ2*CDABS(NSUP)**2
      H0D = DSQRT(H0DSQ)
C
      WIDTH = 0.500D0
```

```
          FLL = FLOAT(LL)
          FMM = FLOAT(MM)
          WT = WIDTH/(FLL)
          WTM = W1/(FMM)
C
      DO 900 I = 1,MM
          P(I) =  FLOAT(I)*WTM
C       NSQ(I) = DCMPLX(-16.D0,.5D0)
900   CONTINUE

      DO 901 I = MM + 1,NN
          P(I) = P(MM) + FLOAT(I-MM)*WT
901   CONTINUE
C
C ENTER REFRACTIVE INDEX DISTRIBUTION
C
      DO 9011 I = 1,NN
          NSQ2(I) = NSQ(NN-I + 1)
C       NSQ(I) = 1.5D0**2
9011  CONTINUE

      DO 9012 I = 1,NN
          NSQ(I) = NSQ2(I)
C       WRITE(17,*)NSQ(I)
```

```
9012  CONTINUE


      DO 977 I = 1,NN
         Q(I) = K*CDSQRT(NSQ(I)-NZSQ)
977   CONTINUE

      QP = K*CDSQRT(NSUPSQ-NZSQ)
      QB = K*CDSQRT(NSUBSQ-NZSQ)

           RHO = NSQ(NN)/NSUBSQ
      A(NN) = 1.D0
      B(NN) = RHO*C*QB/Q(NN)
      DO 129 I = NN,2,-1
           RHO = NSQ(I-1)/NSQ(I)
      A(I-1) = A(I)*CDCOS(Q(I)*(P(I)-P(I-1)))
     $-B(I)*CDSIN(Q(I)*(P(I)-P(I-1)))
      B(I-1) = A(I)*CDSIN(Q(I)*(P(I)-P(I-1)))
     $+B(I)*CDCOS(Q(I)*(P(I)-P(I-1)))
      B(I-1) = B(I-1)*RHO*Q(I)/Q(I-1)
129   CONTINUE
           RHO = NSUPSQ/NSQ(1)
      RATIO = A(1)*CDSIN(Q(1)*P(1)) + B(1)*CDCOS(Q(1)*P(1))
      RATIO = RATIO/(A(1)*CDCOS(Q(1)*P(1))-B(1)*CDSIN(Q(1)*P(1)))
      RATIO = RATIO*RHO*Q(1)/QP/C
```

```
      REFLCO=(1.D0-RATIO)/(1.D0+RATIO)
      H0=(A(1)*CDCOS(Q(1)*P(1))-B(1)*CDSIN(Q(1)*P(1)))
      H0=H0/(1.D0+REFLCO)

      WRITE(16,*) E0DSQ,CDABS((REFLCO)**2)
C     WRITE(6,*) E0DSQ,CDABS(REFLCO)
C
C ADJUST THE FIELD AMPLITUDE
C H0=COMPUTED INCIDENT MAGNETIC FIELD AMPLITUDE
C H0D=DESIRED OR ACTUAL INCIDENT MAGNETIC FIELD AMPLITUDE
C
      DO 729 I=1,NN
        A(I)=(H0D/H0)*A(I)
        B(I)=(H0D/H0)*B(I)
729   CONTINUE

C####################################################
C%%%%%%%%%%%%%%%%%%%%%%%%%%%%%%%%%%%%%%%%%%%%%%%%%%%%%%%%%%
C___________%%%%%%%%%%%%%%%%%%%%%%%%%%%%%%%%___________
C
      E0DSQ=E0DSQ+1.D-5
      IF(E0DSQ.LE..1D-2) GO TO 1111
888   CONTINUE
      WRITE(6,*) 'SEE THE REF VR I IN NR1NL2.REF'
```

```
      WRITE(6,*) 'SEE THE REFRACTIVE INDEX IN NR1NL2.REFIND'
      STOP
      END
```

References

[1] V. M. Agranovich, V. S. Babichenko, and Y. Ya Chernyak. Nonlinear surface polaritons. *Sov. Phys. JETP*, 32:532, 1980.

[2] E. Kretschmann. The determination of the optical constants of metals by the excitation of surface plasmons. *Z. Phys.*, 241:313–324, 1971.

[3] H. Gugger, M. Jurich, J. D. Swalen, and A. J. Sievers. Observation of an index-of-refraction-induced change in the drude parameters of ag films. *Phys. Rev. B*, 30(8):4189, 15 october 1984.

[4] I. Pockrand. Surface plasma oscillation at silver surfaces with thin transparent and absorbing coatings. *Surface Science*, 72:577–588, 1978.

[5] C. Nylander, B. Lindberg, and T. Lind. *Sensors and Actuators*, 3:79, 1982.

[6] B. L. Liedberg, C. Nylander, and I. Lundstorm. *Sensors and Actuators*, 4:299, 1983.

[7] M. T. Flanagan and R. H. Pantell. Surface plasmon resonance and immunosensors. *Electronics Letters*, 20(23):968–970, 8th November 1984.

[8] P. B. Daniels, J. K. Deacon, M. Eddowers, and D. G. Pedel. *Sensors and Actuators*, 15:11, 1988.

[9] B. Moslehi, M. W. Foster, and P. Harvey. Optical magnetic and electric field sensors based on surface plasmon polariton resonant coupling. *Electronic Letters*, 27(11):951–953, 23 May 1991.

[10] E. M. yeatman and M. E. Caldwell. Spatial light modulation using surface plasmon resonance. *Appl. Phys. Lett.*, 55(7):613–615, 14 August 1989.

[11] M. J. Adams. *An introduction to optical waveguides.* John Wiley & Sons, Inc, 1981.

[12] A. D. Boardman. *Electromagnetic surface modes.* John Wiley & Sons, Inc , 1982.

[13] Martin E. Caldwelll and Eric M. Yeatman. Optically addressed surface plasmon spatial light modulators. *SPIE*, 1990.

[14] Andreas Otto. Excitation of nonradiative surface plasma waves in silver by the method of frustrated total reflection. *Zeltschrift for Physik*, 216:398–410, 1968.

[15] M. L. Dakss, L. Kuhan, P. F. Heidrich, and B. A. Scott. *Applied Physics Letters*, 16:523, 1970.

[16] H. Kogelnik and T. P. Sosnowski. *Bell System Technical Journal*, 49:1602, 1970.

[17] T. Tamir. *Integrated optics*. Springer-Verlag Berlin Heidelberg , 1975.

[18] A. R. Neureuther and F. H. Dill. *In Proc. Symp. Optical and Acoustical Micro-Electronics*. Polytechniic Press,New York, 1974.

[19] D. G. Dalgoutte. *Optical Communication*, 8(1):124, 1973.

[20] Benno Rothenhausler and Wolfgang Knoll. Surface-plasmon microscopy. *Nature*, 332:615–617, 14 April 1988.

[21] W. R. Seitz. Chemical sensors based on fiber optics. *Anal. Chem.*, 56:16A, 1984.

[22] L. M. Zhang and D. Uttamchandani. Optical chemical sensing employing surface plasmon resonance. *Electronics Letters*, 24(23):1469–1470, 10th November 1988.

[23] Liang Chi Shen and Jin Au Kong. *Applied electromagnetism*. PWS publishers, 1987.

[24] F. Dios, L. Torner, and F. Canal. Self-consitent solution for general nonlinear slab waveguides. *Optical Communications*, 72(1,2):54–59, 1 July 1989.

[25] S. J. Al-Bader. Tm waves in nonliear saturable thin films: a multilayered approach. *Journal of Lightwave Technology*, 7(4):717–724, April 1989.

[26] Jin Au Kong. *Electromagnetic wave theory.* John Wiley & Sons, Inc, 1986.

[27] S. J. Al-Bader and H. A. Jamid. Guided waves in nonliear saturable self-focusing thin films. *Journal of Quantum Electronics*, QE-23(11):1947–1955, November 1987.

[28] Werner Hickel and Benno Rothenhausler. Surface plasmon microscopic characterization of external surfaces. *J. Appl. Phys.*, 66(10):4832–4836, 15 November 1989.

[29] R. Ulrich. Optimum excitation of optical surface waves. *Journal of the Optical Society of America*, 61(11):1467–1476, November 1971.

[30] R. Reinisch, P. Vincent, and M. Neviere. Fast pockels light modulator using guided wave resonance. *Applied Optics*, 24(13):2001–2004, 1 July 1985.

[31] U. Efron et al. Silicon liquid crystal light valves: status and issues. *Optical Engineering*, 22(6):582–686, Nov./Dec. 1983.

[32] I. Pockrand. Resonance anomalities in the light intensity reflected at silver gratings with dielctric coatings. *J. Phys. D. : Appl. Phys.*, 9:2423–2432, 1976.

[33] Y. J. Chen and G. M. Carter. Measurement of third order nonlinear susceptibilities by surface plasmon. *Appl. Phys. Lett.*, 41(4):307–309, 15 August 1982.

[34] G. I. Stegeman and R. J. Seymour. Surface plasmon attenuation by thin film overlayers in the far infrared. *Solid State Communications*, 44(9):1357–1358, 1982.

[35] Benno Rothenhausler and Wolfgang Knoll. Interferometric determination of the complex wave vector of plasmon surface polarities. *J. Opt. Soc. Am.*, 5(7):1401–1405, July 1988.

[36] Dror Sarid et al. Optical field enhancement by long-range surface-plasma waves. *Applied Optics*, 21(22):3993–3995, 15 November 1982.

[37] Benno Rothenhausler, Claus Duschio, and Wolfgang Knoll. Plasmon surface polartion fields for the characterization of thin films. *The Solid Films*, 159:323–330, 1988.

[38] Eduardo Fontana, R. H. Pantell, and M. Moslehi. Characterization of dielectric-coated, metal mirrors using surface plasmon spectroscopy. *Applied Optics*, 27(16):3334–3340, 15 August 1988.

[39] G. T. Sincerbox and J. C. Gordon. Small fast large-aperture light modulator , using attenuated total reflection. *Applied Optics*, 20(8):1491–1494, 15 April 1981.

[40] E. Yeatman and E. A. Ash. Surface plasmon microscopy. *Electronics Letters*, 23(20):1091–1092, 24th September 1987.

[41] R. Hickernell and D. Sarid. Optical bistability using prism-coupled, long-range surface plasmon. *J. Opt. Soc. Am. B.*, 3(8):1059–1069, August 1986.

[42] Zhan Chen and H. J. Simon. Attenuated total reflectance from a layered silver grationg with coupled surface waves. *J. Opt. Soc. Am. B.*, 5(7):1396–1400, July 1986.

[43] L. Wendler and R. Haupt. An improved virtual mode theory of atr experimentson surface polartion. *Phys. Stat. sol. (b)*, :131–148, 1987.

[44] Helene E. de Brujin et al. Determination of dielectric permitivity and thicjness of a metal layer from a surface plasmon resonance experiment. *Appied Optics*, 29(13):1974–1978, 1 May 1990.

[45] Y. Mao, H. A. Macleod, and K. Balasubramanian. Magnetoptial thin film optical constants measurement using sutface plasmon resonance. *Applied Optics*, 28(14):2914–2917, 15 July 1989.

[46] Koji Matsubara, S. Kawata, and S. Minami. Optical chemical sensor based on surface plasmon measurement. *Applied Optics*, 27(6):1160–1163, 15 March 1988.

[47] W. Hickel and W. Knoll. Surface plasmon optical characterization of lipid monolayers at 5 μ m lateral resolution. *J. Appl. Phys.*, 67(8):3572–3575, 15 April 1990.

[48] E. Fontana, R. H. Pantell, and S. Strober. Surface plasmon immunoassay. *Applied Optics*, 29(31):4694–4704, 1 November 1990.

[49] Eduardo Fontana, R. H. Pantell, and M. Moslehi. Characterization of dielectric-coated, metal mirrors using surface plasmon spectroscopy. *Applied Optics*, 27(16):3334–3340, 15 August 1988.

[50] Eric M. Yeatman and Martin E. Calwell. Surface plasmon spatial light modulators. *SPIE*, 1151:, 1989.

[51] Eric M. Yeatman and Eric A. Ash. Computerized surface plasmon microscop. *SPIE*, 1028:, 1988.